**European Journal of Biophysics**
2016; 4(4): 22-41
http://www.sciencepublishinggroup.com/j/ejb
doi: 10.11648/j.ejb.20160404.11
ISSN: 2329-1745 (Print); ISSN: 2329-1737 (Online)

# A Quantum Field Based Approach to Describe the Global Molecular Dynamics of Neurotransmitter Cycles

**Paul Levi**

Institute for Parallel and Distributed Systems (IPVS), Faculty for Informatics, Electrical Engineering and Information Technology, University Stuttgart, Stuttgart, Germany

**Email address:**
paul.levi@ipvs.uni-stuttgart.de

**To cite this article:**
Paul Levi. A Quantum Field Based Approach to Describe the Global Molecular Dynamics of Neurotransmitter Cycles. *European Journal of Biophysics.* Vol. 4, No. 4, 2016, pp. 22-41. doi: 10.11648/j.ejb.20160404.11

**Received**: September 22, 2016; **Accepted**: October 2, 2016; **Published**: October 27, 2016

**Abstract:** Descriptions of neurotransmitter cycles in chemical synapses are generally accomplished in the field of macroscopic molecular biology. This paper proposes a new theoretical approach to model these cycles with methods of the non-relativistic quantum field theory (QFT) which is applicable on small neurotransmitters of nano size like amino acids or amines. The whole cycle is subdivided into the standard five phases: uptake, axonal transport, release and reception. Our ansatz is concentrated to quantum effects, which are relevant in molecular processes. Examples are quantization of momentums and energies of all small transmitters, definition of the density based quantum information; quantization of molecular currents because densities of generate them quantized particles. Our model of the neurotransmitter cycle of chemical synapses was created by the emphasis of possible essential quantum effects; therefore, we neglect many additional molecular aspects that do not lead us to quantum impacts. We elucidate the ramification of our quantum-based approach by the definition of particular Hamiltonians for each of the five phases and by the calculation of the corresponding molecular dynamics. The transformation from the particle representation to usual wave functions yields the probability to find at the same time n neurotransmitters of different energy states at different positions. Our results have far-reaching implications and may initiate animated discussions. The validation or the disconfirmation of our hypothesis is still open.

**Keywords:** Neurotransmitter Cycle, Small Molecules, Quantum Field Theory, Quantized Energy, Quantized Information

## 1. Introduction

In the past decade spiking neurons received much attention and remarkable progress has been achieved, e.g. in the visualization of multi-dimensional neural connections by the Blue Brain Project [27] and in the development of the NEST simulator [30]. Today, all these efforts are continued and extended by the Human Brain Project (HBP) that is a FET Flagship Project in Horizon 2020. Here, we point out that all these ongoing works can be resumed by the two fundamental characteristics of neurons. At first, we cite their ability to generate firing rates by action potentials. The amplitudes and frequencies of spiking neurons are relevant for the internal presynaptic firing rate and even more essential for the external signal input to the brain and the corresponding pulse trains out of the brain. This topic is also extensively treated in the literature [8], [13], [14]. At second, we name the ability of internal molecular signaling which is based on complex chemical processes, [19], [1], [9], [28]. All above-mentioned research activities to obtain a deeper understanding of the two fundamental neural abilities are usually done on the macroscopic level.

Our contribution is devoted to the description of the synaptic transmission cycle in the framework of molecular biology (second neural ability). However, the main difference of our methodology to the common techniques, which are applied in this field, is the utilization of the operations of the non-relativistic quantum field theory (QFT).

There are two central reasons to elaborate this particular approach. First, the considered small neurotransmitters have a size of around 1nm (amino acids, amines). Hereby, we note that the double-slit effect already has been observed with atoms of equivalent sizes, e.g. for He atoms [22] and for $C_{60}$ atoms [3]. Certainly, both experiments have been performed under vacuum conditions. However, quantum effects also are observed under real, biological conditions, where for

example water, salt, different temperatures and other interacting molecules exist. Examples of quantum effects under such conditions are reported e.g. in the photosynthesis [29] and in the magneto reception of migrant birds [23]. Additional, particular quantum based neural topics are e.g. molecular dynamics in noisy environment [20], quantum processes in the brain concerning consciousness [5], quantum computation [15]. Finally, the well-established discipline of quantum chemistry get new impacts, e.g. by [34], [18], [25].

Second, various applications of the QFT methods are applied in solid-state physics [6], [16] in superconductivity, in elementary particle physics [35] and in super fluidity [31], [11]. Recently, molecules also are handled as nano particles using quantum theory in molecular robotics [32], [17]. Moreover, quantum theory methods are already have been applied to the study of DNA nano robotics [33].

In summary, the application of quantum methods essentially demonstrates that molecules can show wave like aspects (particle wave duality) and the synchronization of a huge amount of molecules by running quantum waves [24]. Furthermore, in biological systems molecular densities, molecular currents, and their dynamics play a dominant role, this is why the particle representation of the QFT is well suited to describe these features.

# 2. Materials and Processes

### *2.1. Materials (Particles)*

Small neurotransmitter are treated as Bosons [36] because many of them have integer spins like amines and in real applications very often only the angular momentum (quantized rotation modes) of molecules are significant. Aside from this remark, we cite in favour of our bosonic conjecture the following two facts. First, Bosons obey the Bose-Einstein-distribution

$$p_{BE}(n_{\boldsymbol{k}}) = \frac{\left(e^{-\beta E_{\boldsymbol{k}}}\right)^{n_{\boldsymbol{k}}}}{Z}. \qquad (1)$$

Here, we have: $n_{\boldsymbol{k}}$ = 0, 1, … defines the number of the released neurotransmitters (eigenvalue of the corresponding particle operator $N_{\boldsymbol{k}}$, where $\boldsymbol{k}$ marks wave number vector) with the defined energy quant $E_{\boldsymbol{k}} = \hbar\omega_{\boldsymbol{k}} = \frac{(\hbar k)^2}{2\mathrm{m}_0}$, $\mathrm{m}_0$ indicates the particle mass, $Z = \frac{1}{1-e^{-\beta E_{\boldsymbol{k}}}}$ denotes the partition function Z, parameter $\beta$ is given by $\frac{1}{k_B T}$, $k_B$ is the Boltzmann constant, T is the temperature in Kelvin. Thus, the mean number of particles $\langle n_{\boldsymbol{k}} \rangle$ with energy $\hbar\omega_{\boldsymbol{k}}$ of a system in thermal equilibrium is calculated by the well-known formula of statistical physics

$$\langle n_{\boldsymbol{k}} \rangle = \sum_{\boldsymbol{k}} n_{\boldsymbol{k}}\, p_{BE}(n_{\boldsymbol{k}}) = \frac{1}{e^{\beta\hbar\omega_{\boldsymbol{k}}-1}}, \qquad (2)$$

where $e^{\beta\hbar\omega_{\boldsymbol{k}}}$ is positive and for lower energies slightly greater as 1. Hence, if we replace in this expression the particular energy $E_{\boldsymbol{k}}$ by the mean energy $\langle E \rangle$ (standard normalization of the energy scale), then we observe that the most particles can be found at the mean energy and only few particles with higher energy (similar to the Boltzmann particle number). While, for Fermions the mean particle number does not ensure such a steady energetic distribution of particles because, the spectrum of these particles is much broader. So, only one particle can be found at the mean energy.

Second, we cannot principally exclude that also Fermions exist in the synaptic cleft. Nevertheless, in consequence the additional integration of Fermions in the Hamiltonians they get dominantly more complex and we have to model the case that two Fermions (e.g. hydrogen molecule $H_2$) or even more Fermions can generate a Boson by spin interactions. Further, also all kinds of spin-spin interaction have to be calculated. Therefore, the analytic complexity of the Hamiltonians and of the corresponding equations of motion dominantly increases and the numerical effort to solve these equations of motion noticeable grows up. Therefore, we consider finally only Bosons in our approach for reasons of simplification and better understandability.

We calculate the typical de Broglie wavelength $\lambda$ of neurotransmitters for simplification in the linear box normalization of the synaptic cleft. Hereby, the momentum is $p = \hbar\, k = \hbar\frac{\pi\, n_k}{L}$. We assume that L = 50 nm (maximal length of the cleft) then this yields $\lambda = \frac{2L}{n_k} = \frac{10^{-9}}{n_k}$ m. The corresponding energy is $E_k = \frac{\hbar^2}{2m_0}\left(\frac{n_k\,\pi}{L}\right)^2$. For clarification, we cite the molecular mass of two typical small mass neurotransmitters: GABA with $m_0$ = 17.18 $10^{-23}$ g and dopamine with $m_0$= 25.63 $10^{-23}$ g. Therefore, the energy for example of a dopamine molecule is $E_k = {n_k}^2\ 769\ 10^{-19}$ J = ${n_k}^2$ 480.6 eV.

For comparison, if we calculate $\lambda$ in the "continuous normalization", where we use the GABA mass and set T equal to the body temperature T = 310.14 K (≈37 ℃) then we get the value $\lambda = \frac{h}{\sqrt{m_0 k_B T}}$ = 2.3 $10^{-9}$ m. This result is of the same order of magnitude as for the box normalization, but $\lambda$ is not quantized.

The differentiation between inhibitory and excitatory chemical synapse will be described by the type of the neurotransmitter molecule, e.g. GABA is an inhibitory transmitter and glutamate an excitatory transmitter, acetylcholine can either excite or inhibit depending on the type of receptor its binds to. In electrical descriptions excitatory neurotransmitter open cation channels, so influx of $Na^+$ depolarize the postsynaptic membrane. Inhibitory neurotransmitters open channels e.g. $K^+$, which reduce the excitatory influence to depolarize the postsynaptic membrane. We mentioned these electrical aspects of polarization and respectively depolarization for reasons of understanding the complexity of the processes of chemical synapses. In this contribution, we only focused on chemical processes, which generate these polarization resp. depolarization effects.

### *2.2. Processes*

This contribution takes up the QFT approach and extends

it to an abstract, global model of the transmission cycle of small sized neurotransmitters in chemical synapses. The whole process is arranged in five phases: loading (uptake) of transmitters in vesicles, their transport along microtubules of a presynaptic axon, the release of neurotransmitters into the synaptic cleft, their transmissions through the synaptic cleft, and finally their reception by particular transmitter−gated ion channels at the postsynaptic plasma membrane. For reasons of simplicity and ease of understanding we concentrate only on cationic channels, neglecting anionic channels and channel regulations by second messengers (G-proteins) [2], [21]. Details of the axonal transport of the vesicles by molecular robots (motor proteins like kinesin, dynein, and myosin) have been already published [24], therefore we exclude in this article the detailed description of the four sub-phases of the axonal transport and condense them in one-step.

Next, we prefer to reason why we have accomplished a global model of the neurotransmitter cycle and do not consider the characteristic features of these five phases. Therefore, one principal goal of our work is the development of a description of a quantized n-particle system on a molecular physics level, which considers only the relevant quantum-based interactions of the particles during the whole neurotransmitter cycle. This decision is apparently understandable if we just consider all relevant processes (interactions) which occur at the presynaptic side, in the synaptic cleft and at the postsynaptic level.

*At presynaptic side*: synthesizing of neurotransmitters, loading of vesicles and the parallel transport along microtubules in both directions (anterograde, retrograde for recycling) involve several steps, the organization of vesicles is complex at the active zone and many proteins interacts with vesicles, the process of the release of neurotransmitters into the cleft requires a number of operations (exocytosis), membrane potentials change (polarization, depolarization), each single vesicle emits about $10^4$ and there are dozens of out spilling vesicles in the active zone, so about $10^6$ transmitters are emitted in milliseconds, etc.

*At the cleft level*: a big amount of neurotransmitters of different types is e.g. congregated together with ions, ion-gates, solutes, salt and water. Therefore, many inter-molecular interactions occur, ions react with ion-gates (proteins), neurotransmitter can be inactivated (enzymatic destruction), support of reuptake into the presynaptic axon terminal is going on, the stabilization of the parallel orientation of the pre synaptic and post synaptic plasma membrane occur, etc.

*At postsynaptic side*: the distribution of receptors is not constant like on a flat screen but it is 3-d curved and clusters of PSD proteins exist, the receptors are mobile, because there are interactions with membrane binding sites, different possibilities exist how ions can permeate channels, diffusion through the extracellular fluid back to presynaptic axon terminal (reuptake), generation of a new action potential (synaptic integration), etc.

It is obvious that the description of the transmission cycle, where all relevant features are considered, is very difficult, ambitious and nearly impossible. Therefore, the most authors model correctly particular processes of this cycle. Thus, we know about the complexity and difficulty to construct a correct, detailed model of the transmission cycle, therefore we pursue the direction to evaluate a more abstract n-particle system with appropriate interactions of all five-transmission phases. The main impact to proceed this way is given by the elicitation of the one important point: quantum effects can characterize the transmission cycle and in consequence of these effects the density matrix $\rho$ and the biological relevant information ($-\rho \ln\rho$) are also quantized at the level of particle numbers. This means that in all five phases particular interactions procced considerably different as it is usually reported. Nevertheless, the most processes described above (presynaptic level, etc.) are not relevant with respect to quantum biology, therefore we disregarded them.

# 3. Methods

For each of the five phases (with exception of the approaches: multiple scattering and diffusion in phase 4) we define at first the corresponding Hamiltonian $H_{int}$ in the interaction representation which allow us to neglect the Hamiltonian for free particles, e.g. $H_0 = \sum_{\boldsymbol{k}} \hbar\omega_k nt_{\boldsymbol{k}}^{\dagger} nt_{\boldsymbol{k}}$, where the operator $nt_{\boldsymbol{k}}^{\dagger}$ creates a neurotransmitter and $nt_{\boldsymbol{k}}$ annihilates an neurotransmitter. We utilize the box normalization, with discrete wave vectors $\boldsymbol{k}$ (e.g. see above the de Broglie wavelength). Afterwards, the resulting equations of motion are presented in the Heisenberg picture

$$\frac{d}{dt}O = \frac{i}{\hbar}\,[H_{int}, O] - \gamma O - F_O, \tag{3}$$

where $O(\boldsymbol{x}, t)$ is a time-dependent operator, and $[H_{int}, O]$ denotes a commutator. In addition, the full equation (3) can be supplemented by a damping constant $\gamma$ and by fluctuating forces $F_O$. However, since we are looking for solutions of our equations of motion in form of expectation values we will abandon the fluctuating force in all corresponding equations because their expectation values are zero.

The solutions of the equations of motions of all five phase are mostly numerically calculated and diagrammed by figures. Exceptions of this approach only occur in the transmission phase (phase 4), where we also present analytic solutions.

# 4. Results

### *4.1. First Phase: Loading*

*Hamiltonian of the loading phase*

The load of neurotransmitters on a microtubule denotes the first step of this phase by molecular robots. That is, we introduce three different creation operators (indicated by a dagger †) and their corresponding annihilation operators. First, we define the creation operator of a molecular robot (motor protein) $r_{x_l,k_r}^{\dagger}$ which operates as a carrier protein and is specified by its discrete position $\boldsymbol{x}_l$ $(l = 1, \ldots, N_l)$ on a microtubule (lane) as a part of the axon of the presynaptic

side and its wavenumber vector $\boldsymbol{k}_r$. Second, we need a container in which the cargo is carried. The suitable container is a vesicle, which is created by the operator $v^\dagger_{x_l}$. The subscript $\boldsymbol{x}_l$ specifies its actual lane position. Third, we have to consider the cargo, which is loaded in a vesicle. Obviously, the loads are neurotransmitters. The corresponding operator $nt^\dagger_{m_{tr},\boldsymbol{x}_j,\boldsymbol{k}_j}$ creates a neurotransmitter of particular molecular type $m_{tr}$, ($tr$ = 1, …, $n$) at the spatial location $\boldsymbol{x}_j$, with the wavenumber vector $\boldsymbol{k}_j$. The molecular type $m_{tr}$ of a neurotransmitter opens transmitter – gated channels of suited receptors. The subscript $j$ denotes the position and respectively the wave number vector of an individual neurotransmitters of type $m_{tr}$; simply expressed, it enumerates neurotransmitters of the same type.

The product of the vesicle creation operator and $n$ annihilation operators of neurotransmitters

$$v^\dagger_{x_l}\, nt_{m_{tr},x_1,k_1} \dots nt_{m_{tr},x_n,k_n} \tag{4}$$

depicts the loading of the vesicle with $n$ neurotransmitters at the microtubule position $\boldsymbol{x}_l$. The operator product

$$r^\dagger_{x_l,k_r} v^\dagger_{x_l}\, nt_{m_{tr},x_1,k_1} \dots nt_{m_{tr},x_n,k_n} \tag{5}$$

complements the loading process. At the same time, a transport robot $r^\dagger_{x_l,k_r}$ and a vesicle are both created $v^\dagger_{x_l}$ at the lane position $\boldsymbol{x}_l$ and all neurotransmitters are annihilated. The Hermitian conjugate of this operator product models the unloading activity (reverse process). Thus, the complete interaction Hamiltonian reads

$$H^{load}_{int}/\hbar = i g_{lo} \sum_{tr,\boldsymbol{k}_r,x_l,\{x_j,\boldsymbol{k}_j\},r,l} \left( r^\dagger_{x_l,k_r} v^\dagger_{x_l}\, nt_{m_{tr},x_1,k_1} \dots nt_{m_{tr},x_n,k_n} - nt^\dagger_{m_{tr},x_n,k_n} \dots nt^\dagger_{m_{tr},x_1,k_1} v_{x_l} r_{x_l,k_r} \right) \tag{6}$$

The coupling constant $g_{lo}$ parametrizes the load phase. The individual molecular robots $r^\dagger_{\boldsymbol{k}_r,x_l}$ operate at different, discrete lane positions $\boldsymbol{x}_l$.

*Equations of motion of the loading phase*

The equations of motion of the three relevant operators of the loading phase and the time dependence of the molecular density are given by the equations (7) to (9).

$$\dot{r}^\dagger_{x_q,k_r} = g_{lo} \sum_{tr,\boldsymbol{k}_r,\{x_j,\boldsymbol{k}_j\}} nt^\dagger_{m_{tr},x_1,k_1} \dots nt^\dagger_{m_{tr},x_n,k_n} v_{x_q} - \gamma_r r^\dagger_{x_q,k_r}. \tag{7}$$

The dynamics of a molecular robot during the loading is obtained by the creation of the neurotransmitters load and the annihilation of the wrapping vesicle.

$$\dot{v}^\dagger_{x_q} = g_{lo} \sum_{tr,k_r,\{x_j,k_j\}} nt^\dagger_{m_{tr},x_1,k_1} \dots nt^\dagger_{m_{tr},x_n,k_n} r_{x_q,k_r} - \gamma_v v^\dagger_{x_q}. \tag{8}$$

The temporal change of the vesicle state is denoted by the creation of its molecular cargo and the annihilation of the transporting molecular robot.

$$\dot{nt}^\dagger_{m_{tr},x_1,k_1} = -g_{lo} \sum_{tr,\boldsymbol{k}_r,x_2,\boldsymbol{k}_2;\dots;x_n,\boldsymbol{k}_n,r,l} nt_{m_{tr},x_2,k_2} \dots nt_{m_{tr},x_n,k_n}\, r^\dagger_{x_l,k_r}\, v^\dagger_{x_l} - \gamma_{nt} nt^\dagger_{m_{tr},x_q,k_q} \tag{9}$$

The dynamics of a particular neurotransmitter is characterized by the annihilation of all other transmitters (except the first one) and the simultaneous creation of a molecular robot together with a vesicle, both at the same position.

The three solutions (7) to (9) show a compliant behavior. After some oscillations at the beginning, they converge towards a stable fixed point. Such a common property is well reproduced by a phase diagram. Figure 1 shows the collective trajectory of the real part (red) and imaginary part (blue) of all three variables, where both parts start at the same position and end at another equal location.

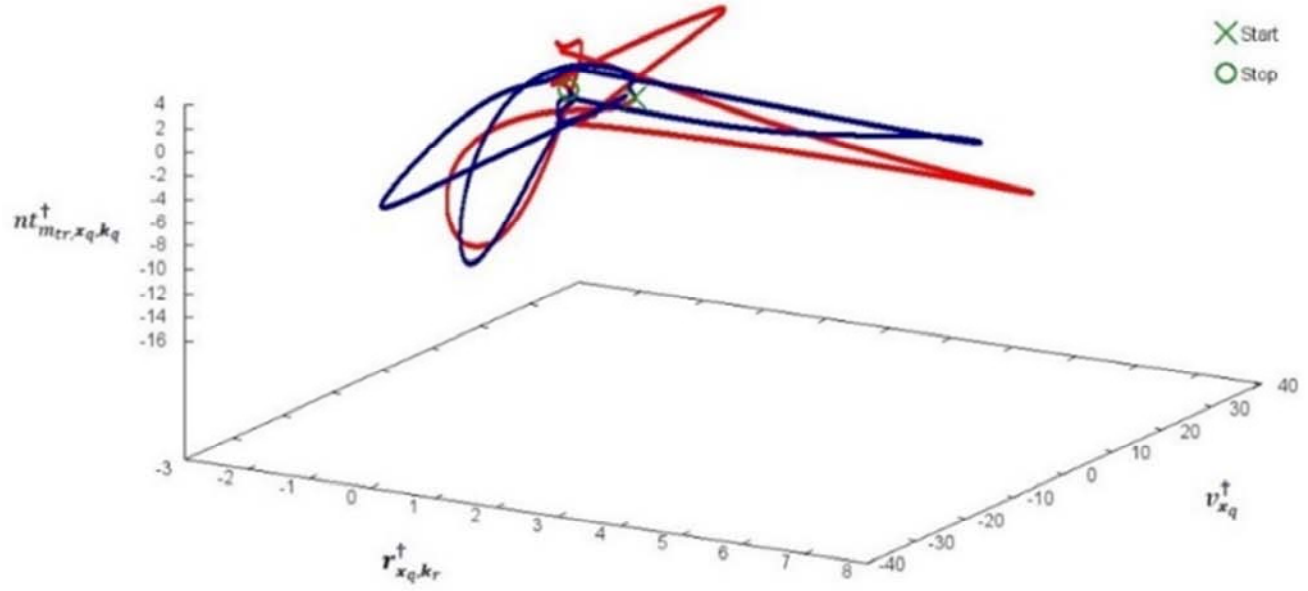


***Figure 1.*** *Phase diagram of the real part (red) and the imaginary part (blue) of the three variables $r^\dagger_{x_q,k_r}$, $v^\dagger_{x_q}$ and $nt^\dagger_{m_{tr},x_q,k_q}$ (equations (7) to (9)). The common damping constant is $\gamma = 0.175$.*

The equation of motion of the density of the loaded neurotransmitters is given by

$$\frac{d}{dt}\left( nt^{\dagger}_{m_{tr},\boldsymbol{x}_1,\boldsymbol{k}_1} nt_{m_{tr},\boldsymbol{x}_q,\boldsymbol{k}_1}\right) = -g_{lo} \sum_{tr,\boldsymbol{k}_r,\boldsymbol{x}_2,\boldsymbol{k}_2;\ldots;\boldsymbol{x}_n,\boldsymbol{k}_n,r,l} \; r^{\dagger}_{\boldsymbol{x}_l,\boldsymbol{k}_r} v^{\dagger}_{\boldsymbol{x}_l} nt_{m_{tr},\boldsymbol{x}_q,\boldsymbol{k}_q} nt_{m_{tr},\boldsymbol{x}_2,\boldsymbol{k}_2} \ldots nt_{m_{tr},\boldsymbol{x}_n,\boldsymbol{k}_n} - g_{lo} \sum_{tr,\boldsymbol{k}_r,\boldsymbol{x}_2,\boldsymbol{k}_2;\ldots;\boldsymbol{x}_n,\boldsymbol{k}_n,r,l} \; nt^{\dagger}_{m_{tr},\boldsymbol{x}_q,\boldsymbol{k}_q} nt^{\dagger}_{m_{tr},\boldsymbol{x}_2,\boldsymbol{k}_2} \ldots v_{\boldsymbol{x}_l} r_{\boldsymbol{x}_l,\boldsymbol{k}_r} \; - \gamma_{nt}(nt^{\dagger}_{m_{tr},\boldsymbol{x}_q,\boldsymbol{k}_q} nt_{m_{tr},\boldsymbol{x}_q,\boldsymbol{k}_q}) \quad (10)$$

A competitive balance between the first term (loading) and its reverse (unloading) characterizes the dynamics of equation (10). Figure 2 demonstrates this time-dependent behavior. Following two oscillations the real part (red) and imaginary part (blue) of the density remain stable and converge to the attractive fixed point zero.

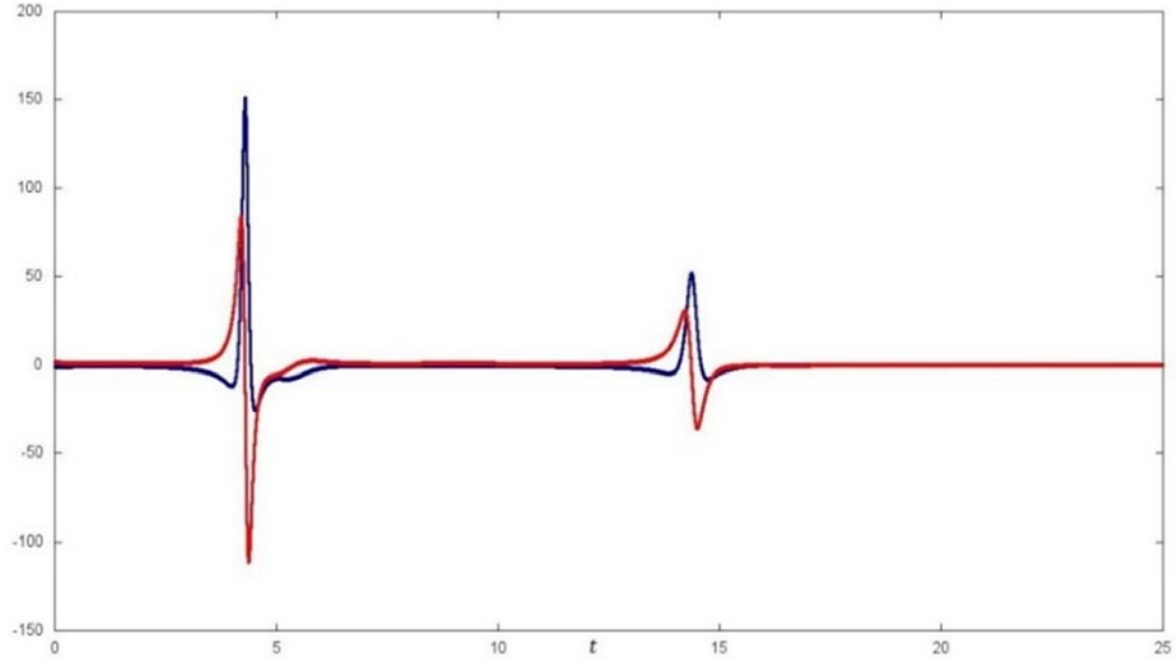


***Figure 2.*** *Trajectory of the real part (red) and imaginary part (blue) of the density of neurotransmitter during the loading phase (equation (10)). The parameters are:* $g_{lo} = 0.1, \gamma_{nt} = 0.19$. *The scale of time axis is characteristic for the loading process, here the numerical value 25 corresponds approximately 1s.*

### *4.2. Second Phase: Axonal Transport*

*Hamiltonian of the axonal transport*

The second phase marks the anterograde axonal transport of neurotransmitters along a microtubule. Here, an individual molecular robot $r^{\dagger}_{\boldsymbol{x}_l,\boldsymbol{k}_r}$ which is loaded with an attached and filled vesicle $v_{\boldsymbol{x}_l}$ moves from the inner lane position $\boldsymbol{x}_l$ to the outer lane position at the releasable compartment $\boldsymbol{x}_o$ $(l < o;\ l, o = 1, \ldots, N_l)$. The following Hamiltonian characterizes this axonal transport

$$H^{ax.-transp.}_{int}/\hbar = \sum_{tr,\boldsymbol{k}_r,\boldsymbol{k}_r',\boldsymbol{x}_o,\{\boldsymbol{x}_j,\boldsymbol{k}_j;\boldsymbol{x}_j',\boldsymbol{k}_j'\},r,o,l} \; r^{\dagger}_{\boldsymbol{x}_o,\boldsymbol{k}_r'} v^{\dagger}_{\boldsymbol{x}_o} nt^{\dagger}_{m_{tr},\boldsymbol{x}_n',\boldsymbol{k}_n'} \ldots nt^{\dagger}_{m_{tr},\boldsymbol{x}_1',\boldsymbol{k}_1'} \quad (11)$$

$$\mathrm{T}\left(\boldsymbol{k}_r', \boldsymbol{x}_n', \boldsymbol{k}_n' \ldots \boldsymbol{x}_1', \boldsymbol{k}_1'; \boldsymbol{k}_r, \boldsymbol{x}_1, \boldsymbol{k}_1 \ldots \boldsymbol{x}_n, \boldsymbol{k}_n\right) \; nt_{m_{tr},\boldsymbol{x}_1,\boldsymbol{k}_1} \ldots nt_{m_{tr},\boldsymbol{x}_n,\boldsymbol{k}_n} v_{\boldsymbol{x}_l} r_{\boldsymbol{x}_l,\boldsymbol{k}_r}.$$

Here, T describes the transfers between all individual triples $(\boldsymbol{k}_r, \boldsymbol{x}_j, \boldsymbol{k}_j)$ and $\left(\boldsymbol{k}_r', \boldsymbol{x}_j', \boldsymbol{k}_j'\right), j = 1, 2, \ldots, n$. That is, T enforces the nearest neighbor restrictions (interactions) for each pair of individual triples:

$$\mathrm{T}\left(\boldsymbol{k}_r', \boldsymbol{x}_j', \boldsymbol{k}_j'; \boldsymbol{k}_r, \boldsymbol{x}_j, \boldsymbol{k}_j\right) \neq 0, \text{ if } \boldsymbol{k}_r' \leq \varepsilon_{\boldsymbol{k}_r}, \left|\boldsymbol{x}_j' - \boldsymbol{x}_j\right| \leq \varepsilon_{\boldsymbol{x}_{tr}}, \quad (12)$$

$$\left|\left(\boldsymbol{k}_r', \boldsymbol{x}_j', \boldsymbol{k}_j'\right), -\boldsymbol{k}_j\right| \leq \varepsilon_{\boldsymbol{k}_{tr}} \text{ and } \boldsymbol{x}_j' \neq \boldsymbol{x}_j; \forall\, j,$$

where both kinds of the epsilons are given by $\varepsilon_{\boldsymbol{x}_{tr}} \approx 2\text{nm}$ and $\varepsilon_{\boldsymbol{k}_{tr}} \approx \frac{\pi}{L}$. Thus, a cluster of neurotransmitters should be concentrated to a restricted, spatial region and governed by a very narrow range of allowed momenta.

These restrictions are given in a form, which is well suited if the solutions of the equations of motion of the corresponding Hamiltonian (11) are numerically calculated, which the standard use of this work is. In a classical physical view, T may be compared with two strong attractive potentials in the $\boldsymbol{x}$-space and $\boldsymbol{k}$ space, (see e.g. (28)).

These requirements ensure that after the axonal transport

all neurotransmitters remain in a very restricted spatial and momentum cluster. This bounded cluster property of neurotransmitters is essential for the simultaneous directed release of them into the synaptic cleft and their following transmission to the postsynaptic receptors. The nearest neighbor requirement is significant for the biologically correct description of the transmission and respectively e.g. for diffusion processes to the postsynaptic plasma membrane, because all transmitters are released at once in a close bounded cluster.

*Equations of motion of the axonal transport*

Its motion to the outer position $\boldsymbol{x}_o$ and the change of its wave vector determines the dynamics of the molecular robot. At this new position a new vesicle is created together with the carried neurotransmitters. The vesicle and its load are annihilated at their previous locations.

$$\dot{r}^{\dagger}_{x_q,k_r} = i\sum_{tr,k_r,k'_r,\{x_j,k_j;x'_j,k'_j\},r,o} r^{\dagger}_{x_o,k'_r}\, v^{\dagger}_{x_o}\; nt^{\dagger}_{m_{tr},x'_n,k'_n} \dots nt^{\dagger}_{m_{tr},x'_1,k'_1} \tag{13}$$

$$\mathrm{T}\; nt_{m_{tr},x_1,k_1} \dots nt_{m_{tr},x_n,k_n} v_{x_q} - \gamma_r r^{\dagger}_{x_q,k_r}.$$

The temporal behavior of the vesicle is governed by the creation of a molecular robot and a new vesicle with its corresponding cargo of loaded neurotransmitters at the new position $\boldsymbol{x}_o$ . The molecular robot with the original coefficients $(\boldsymbol{x_q}, \boldsymbol{k}_r)$ and the original neurotransmitters are annihilated

$$\dot{v}^{\dagger}_{x_q} = i\sum_{tr,k_r,k'_r,\{x_j,k_j;x'_i,k'_i\},r,o} r^{\dagger}_{x_o,k'_r}\, v^{\dagger}_{x_o}\, nt^{\dagger}_{m_{tr},x'_n,k'_n} \dots nt^{\dagger}_{m_{tr},x'_1,k'_1} \tag{14}$$

$$\mathrm{T}\; nt_{m_{tr},x_1,k_1} \dots nt_{m_{tr},x_n,k_n} r_{x_q,k_r} - \gamma_v v^{\dagger}_{x_q}.$$

The dynamics of a neurotransmitter is described by the creation of the molecular robot and the vesicle at a new position and the annihilation of these two entities at their original position. The neurotransmitters are annihilated at their previous locations and restored at new positions together with new wave vectors.

$$\dot{nt}^{\dagger}_{m_{tr},x_{tr_q},k_{tr_q}} = i\sum_{tr,k_r,k'_r,\{x_j,k_j;x'_i,k'_i\},r,o,l} r^{\dagger}_{x_o,k'_r} v^{\dagger}_{x_o}\; nt^{\dagger}_{m_{tr},x'_n,k'_n} \dots\; nt^{\dagger}_{m_{tr},x'_q,k'_q} \tag{15}$$

$$\mathrm{T}\; nt_{m_{tr},x_2,k_2} \dots nt_{m_{tr},x_n,k_n} r_{x_l,k_r}\, v_{x_l} - \gamma_{nt}\, nt^{\dagger}_{m_{tr},x_q,k_q}.$$

Figure 3 summarizes in a phase diagram the behaviors of the real part (red) and imaginary part (blue) of all three solutions (13) to (15) during the axonal transport. As in figure 1, both trajectories start at one common point end jointly at another location.

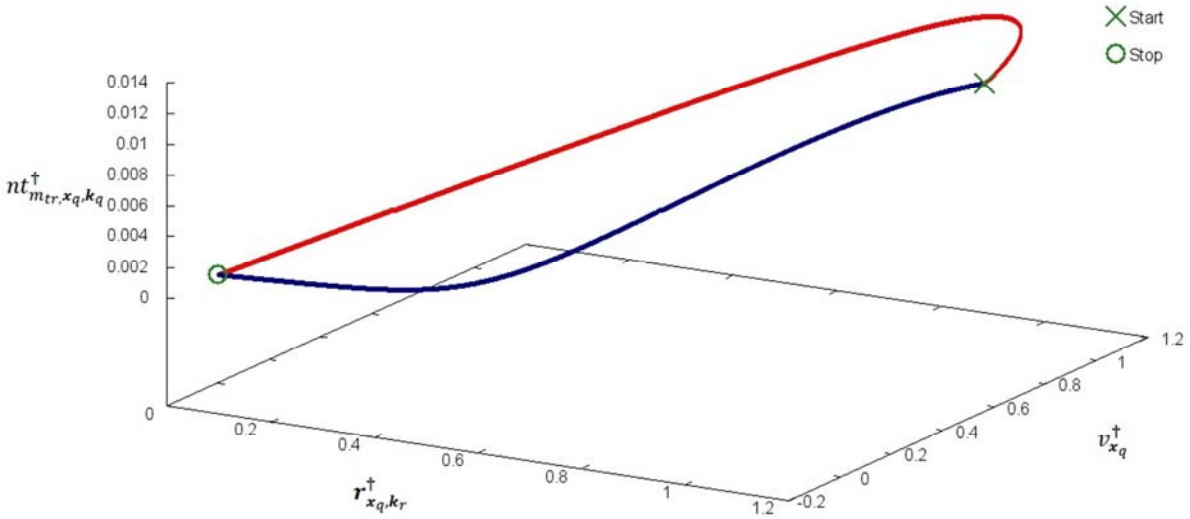


***Figure 3.*** *Phase diagram of the real part (red) and the imaginary part (blue) of the three variable $r^{\dagger}_{x_q,k_r}$, $v^{\dagger}_{x_q}$ and $nt^{\dagger}_{m_{tr},x_q,k_q}$ (equations (13) to (15)). The common damping constant is set to $\gamma = 0.001$.*

The temporal derivative of the density of neurotransmitters at position $\boldsymbol{x}_q$ and wave vector $\boldsymbol{k}_q$ governs the interplay of two different simultaneous processes. One process is responsible for the annihilation of a molecular robot together with a vesicle and the creation of the neurotransmitters. The second process denotes the reverse process.

$$\frac{d}{dt}\left( nt^{\dagger}_{m_{tr},x_q,k_q} nt_{m_{tr},x_q,k_q}\right) = \tag{16}$$

$$\sum_{tr,k_r,k'_r,x_o,\{x_j,k_j;x'_i,k'_i\},r,o,l} \mathrm{T}\left( r_{x_l,k_r}\, v_{x_l}\; nt^{\dagger}_{m_{tr},x'_q,k'_q} \dots\; nt^{\dagger}_{m_{tr},x'_n,k'_n} \right.$$

$$\left. -r^{\dagger}_{x_o,k'_r} v^{\dagger}_{x_o}\; nt_{m_{tr},x_q,k_q} nt_{m_{tr},x_2,k_2} \dots nt_{m_{tr},x_n,k_n}\right) -$$

$$\gamma_{nt}\, nt^{\dagger}_{m_{tr},x_q,k_q} nt_{m_{tr},x_q,k_q}.$$

Figure 4 shows the temporal variation of the real part (red) and imaginary part (blue) of the density of neurotransmitters to which there are ruled. Both parts continuously converge to the fixed point 0 without showing any effect e.g. of a saddle point bifurcation.

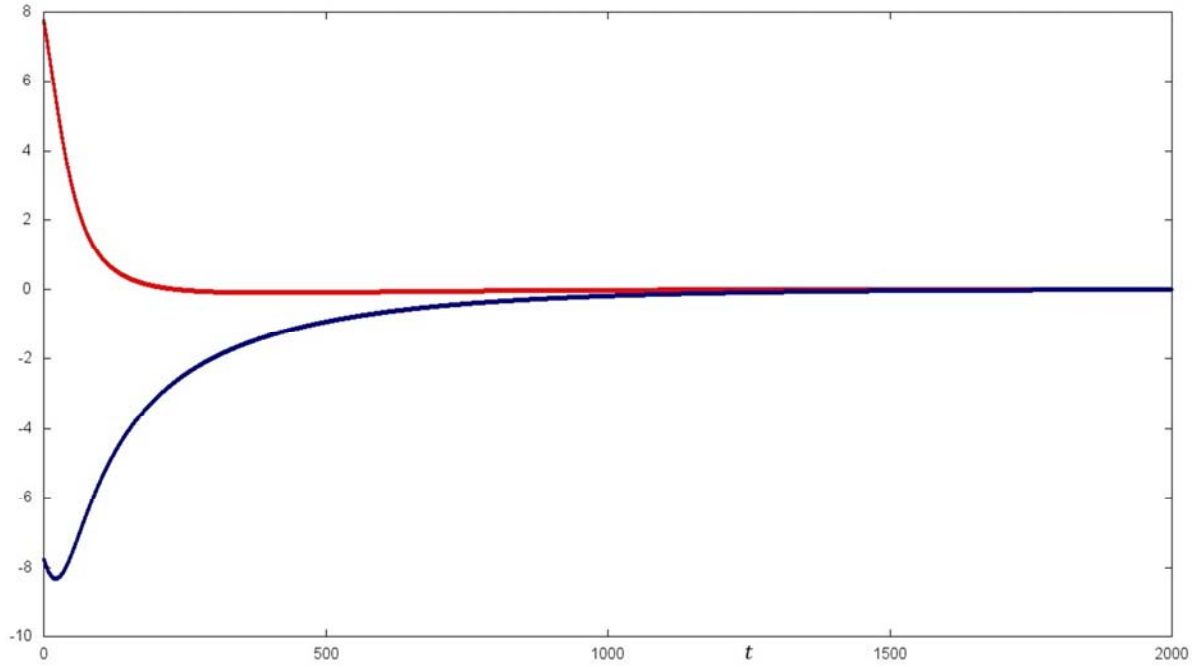


***Figure 4.*** *Dynamics of the density of neurotransmitters (equation (16)) during the axonal transport. The real part is marked by red, the imaginary part is sketched in blue. The damping constant is* $\gamma_{nt} = 0.001$. *The scale of time axis is characteristic for the transport process, here 2000 corresponds approximately 50 ms/h.*

### *4.3. Third Phase: Release*

*Hamiltonian of the release phase*

The first activity of the second phase describes the release of neurotransmitters into the synaptic cleft. This means the combination of the emission of the vesicle-bound neurotransmitters into the cleft and the opening of a cationic channel e.g. a $Ca^{2+}-$ channel. The open channel allows inflow into the active region of the pre $Ca^{2+}-$ synapsis (exocytosis). The impact of such channel operators are denoted by $cach^{\dagger}_{\boldsymbol{x_o}}$ and $cach_{\boldsymbol{x_o}}$ which act at the axonal final position $\boldsymbol{x}_o$.

The release interaction Hamiltonian reads

$$H^{rel.}_{int}/\hbar = ig_{rel}\sum_{tr,\boldsymbol{k}_r,\boldsymbol{x}_o,\{\boldsymbol{x}_j,\boldsymbol{k}_j\},r,o}\left(r^{\dagger}_{\boldsymbol{x}_o,\boldsymbol{k}_r}v^{\dagger}_{\boldsymbol{x}_o}\,cach_{\boldsymbol{x}_o}\mathrm{R}\,nt_{m_{tr},\boldsymbol{x}_1,\boldsymbol{k}_1}\ldots nt_{m_{tr},\boldsymbol{x}_n,\boldsymbol{k}_n} - \mathrm{R}\,nt^{\dagger}_{m_{tr},\boldsymbol{x}_n,\boldsymbol{k}_{m_{tr_n}}}\ldots nt^{\dagger}_{m_{tr},\boldsymbol{x}_1,\boldsymbol{k}_1}cach^{\dagger}_{\boldsymbol{x}_o}v_{\boldsymbol{x}_o}r_{\boldsymbol{x}_o,\boldsymbol{k}_r}\right) \quad (17)$$

where $g_{rel}$ is the coupling constant, which is assigned to the release phase. Compared with the loading Hamiltonian $H^{load}_{int}/\hbar$ we extend this Hamiltonian by two channel operators $cach^{\dagger}_{\boldsymbol{x}_o}$ and respectively $cach_{\boldsymbol{x}_o}$. In addition to the condition (3.9), we require that for all released transmitters similar restrictions are fulfilled:

$$\mathrm{R}\left(\boldsymbol{x}_j,\boldsymbol{k}_j;\ \boldsymbol{x}_{j+1},\boldsymbol{k}_{j+1}\right) \neq 0; j = 1,2,\ldots,n \quad (18)$$

if each pair of the released transmitters fulfills the two conditions:

$$\left|\boldsymbol{x}_j - \boldsymbol{x}_{j+1}\right| \leq \varepsilon_{\boldsymbol{x}} = 2\mathrm{nm} \text{ and } \left|\boldsymbol{k}_j - \boldsymbol{k}_{j+1}\right| = \varepsilon_{\boldsymbol{k}} = 1.$$

Both epsilons ensure that only direct neighbors are considered.

The whole cluster of the emitted ("ejected") transmitters unalterably stays in a very restricted, spatial region and does not spread out in "all" directions. This requirement is expressed by the two following suprema

$$\sup\{\left|\boldsymbol{x}_i - \boldsymbol{x}_j\right|, i \neq j\} = \varepsilon_{\boldsymbol{x}}, \sup\{\left|\boldsymbol{k}_i - \boldsymbol{k}_j\right|, i \neq j\} = \varepsilon_{\boldsymbol{k}}. \quad (19)$$

The release process can also be considered as the simultaneous, multiple outgoing of plane matter waves. Due the fact that the $k$-value are approximately continuously distributed within a small k-interval, the plane wave can superpose to a wave packet. However, the surrounding environment operate as a heat-bath, which cause damping and fluctuations. Therefore, we assume that a wave packet will dissolve and therefore will not represent a coherent state (motion). However, we do not exclude that the wave packet can remain stable and then represents a coherent state.

*Equations of motion of the release phase*

This step is characterized by four equations, which describe the temporal derivatives of the operators representing molecular robots, neurotransmitters, vesicles and channels.

The dynamics of a molecular transport robot is characterized by the simultaneously generation of $n$ neurotransmitters together with the simultaneous opening of a $Ca^{2}_{+}$ channel ($cach^{\dagger}_{\boldsymbol{x_q}}$) and the annihilation of the cargo containing vesicle ($v_{\boldsymbol{x_q}}$).

$$\dot{r}^{\dagger}_{x_q,k_r} = g_{rel} \sum_{tr,k_r,\{x_j,k_j\},r} \mathrm{R}\, nt^{\dagger}_{m_{tr},x_1,k_1} \ldots nt^{\dagger}_{m_{tr},x_n,k_n}\, cach^{\dagger}_{x_q} v_{x_q} - \gamma_r r^{\dagger}_{x_q,k_r}. \tag{20}$$

The time-dependent activities of an individual neurotransmitter is influenced by the coincident generation of all remaining molecules, the opening of a channel and the destruction of the corresponding vesicle and molecular robot, where all these activities occur at the same location $\boldsymbol{x}_o$.

$$\dot{nt}^{\dagger}_{m_{tr},x_q,k_q} = g_{rel} \sum_{tr,k_r,\{x_j,k_j\},r,o} r^{\dagger}_{x_0,k_r} v^{\dagger}_{x_0}\, cach_{x_o} \mathrm{R}\, nt_{m_{tr},x_2,,k_2} \ldots nt_{m_{tr},x_n,,k_n} - \gamma_{nt} nt^{\dagger}_{m_{tr},x_q,k_q}. \tag{21}$$

The equation of motion of the creator $v^{\dagger}_{x_q}$ of a vesicle takes the form

$$\dot{v}^{\dagger}_{x_q} = g_{rel} \sum_{tr,k_r,\{x_j,k_j\},r} \mathrm{R}\, nt^{\dagger}_{m_{tr},x_n,k_n} \ldots nt^{\dagger}_{m_{tr},x_1,k_1} cach^{\dagger}_{x_q}\, r_{x_q,k_r} - \gamma_v v^{\dagger}_{x_q}. \tag{22}$$

The creator of an open $Ca^{2}_{+}$- channel operates according to the following equation

$$\dot{cach}^{\dagger}_{x_q} = -g_{rel} \sum_{tr,k_r,\{x_j,k_j\},r} r^{\dagger}_{x_q,k_r} v^{\dagger}_{q} \mathrm{R}\, nt_{m_{tr},x_1,k_1} \ldots nt_{m_{tr},x_n,k_n} - \gamma_{cach}\, cach^{\dagger}_{x_q}. \tag{23}$$

Figure 5 collects the behaviors of the solutions (real part (red) and imaginary part (blue)) of the three equations (21) to (23) in a phase diagram. Both parts start together at the same position and end up at a same location. This show again the behavior of the attraction of a fixed point. If the damping constant is decreased we observe the same principal behavior but with dominantly more oscillations.

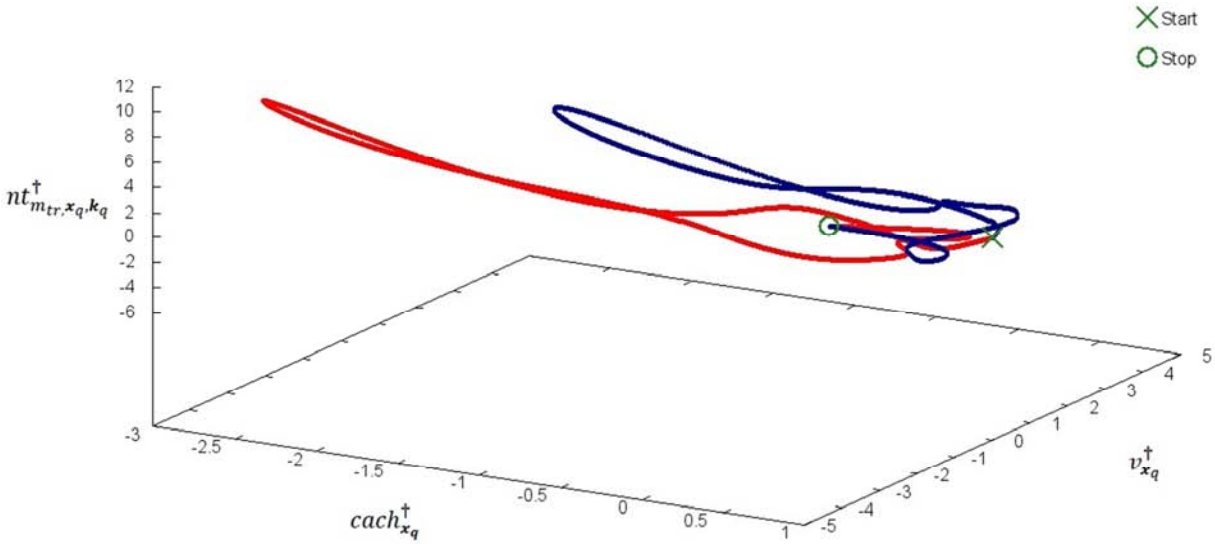


***Figure 5.*** *Phase portrait of the three variables $nt^{\dagger}_{m_{tr},x_q,k_q}$, $v^{\dagger}_{x_q}$ and $cach^{\dagger}_{x_q}$ during the release phase (equations (21) to (23)). The real part is marked by red; the imaginary part is labeled by blue. The collective damping constant is $\gamma = 0.145$, the damping constant gets the value $g_{rel} = 0.1$.*

Equation (24) demonstrates the temporal change of the density of a neurotransmitter at position $\boldsymbol{x}_q$ with wave vector $\boldsymbol{k}_q$, which is characterized by the competition of two processes. The first process denotes the creation of a molecular robot together with a vesicle and the simultaneous annihilation of the channel together with the neurotransmitters. The second process delineates the reverse process. Figure 6 portrays the time-dependent trajectories of the real and imaginary parts of the density of the neurotransmitters during the release step. At the "peak position", the real part (red) goes up, and then it goes down and return to the null line. The trajectory of imaginary part (blue) shows a reverse course.

$$\frac{d}{dt}\left(nt^{\dagger}_{m_{tr},x_q,k_q} nt_{m_{tr},x_q,k_q}\right) = g_{rel} \sum_{tr,k_r,x_o,\{x_j,k_j\},r,o} \left( r^{\dagger}_{x_o,k_r}\, v^{\dagger}_{x_o}\, cach_{x_o} \mathrm{R}\, nt_{m_{tr},x_q,k_q} nt_{m_{tr},x_2,k_2} \ldots nt_{m_{tr},x_n,k_n} \right. \tag{24}$$

$$\left. g_{rel} \sum_{tr,k_r,x_o,\{x_j,k_j\},r,o} \left( r^{\dagger}_{x_o,k_r}\, v^{\dagger}_{x_o}\, cach_{x_o} \mathrm{R}\, nt_{m_{tr},x_q,k_q} nt_{m_{tr},x_2,k_2} \ldots nt_{m_{tr},x_n,k_n} \right.\right.$$

$$+r_{x_o,k_r}\, v_{x_o} cach^{\dagger}_{x_o} \mathrm{R}\, nt^{\dagger}_{m_{tr},x_q,k_q} \ldots nt^{\dagger}_{m_{tr},x_n,k_n}\Big) - \gamma_{nt} nt^{\dagger}_{m_{tr},x_q,k_{trq}} nt_{m_{tr},x_q,k_q}.$$

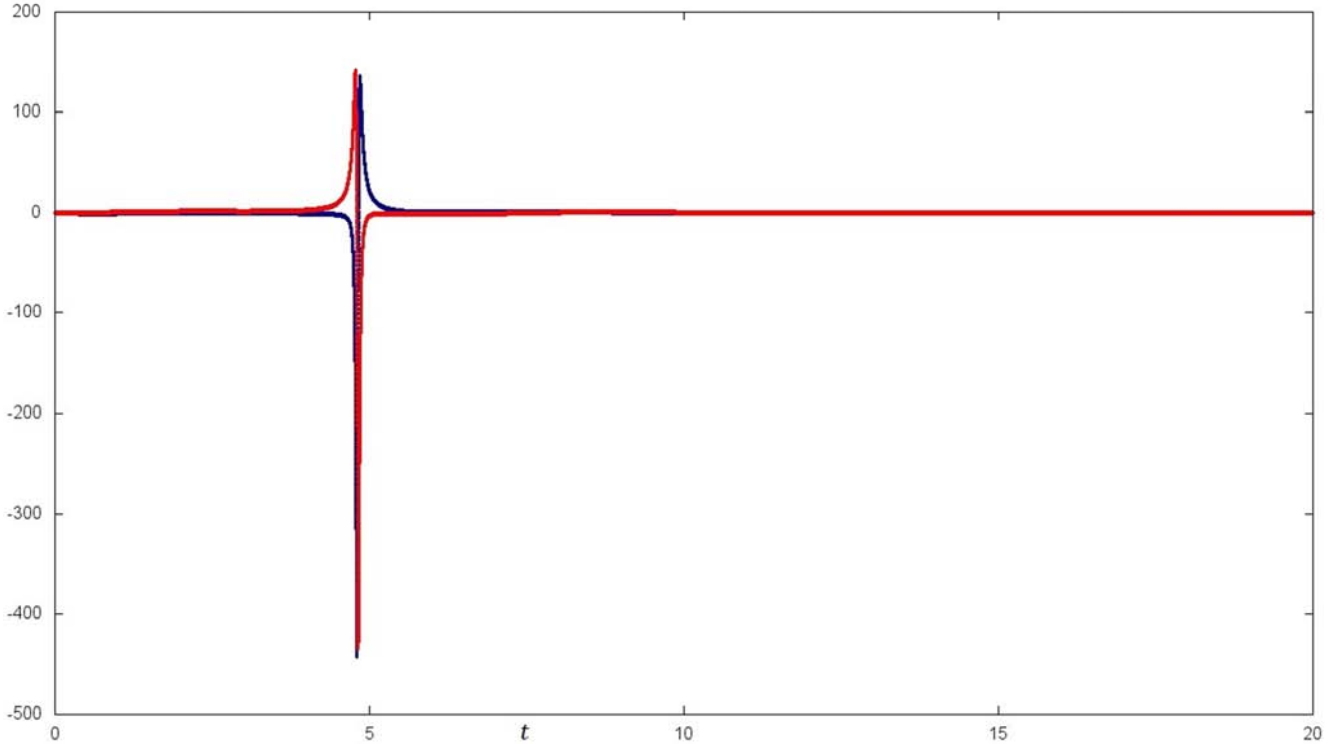


***Figure 6.*** *Dynamics of the density of neurotransmitters (equation (24)) which happens during the release phase (real part: red; imaginary part: blue). The damping constant is set to* $\gamma_{nt} = 0.145$*, the coupling constant takes the value* $g_{rel} = 0.1$*. The scale of time axis is characteristic for the release process; here the numerical value 20 corresponds approximately 5 ms.*

### *4.4. Fourth Phase: Transmission*

The fourth phase is devoted to the transmission of the neurotransmitters through the synaptic cleft. This process is essential and complex therefore we present three essential solutions for this process: multiple scattering, quantum-diffusion and n-particle probability amplitude.

## Approach 1: Multiple Scattering

The scattering process will be considered in the light of quantum effects, which denote wave phenomena. A scattered molecule experiences an interaction at a local potential, where such a process can be described by the perturbation theory of non-relativistic Green´s functions [12], [35]. The Green´s function for free Bosons is defined by

$$G_0(\boldsymbol{x}_e, t_e;\, \boldsymbol{x}_0, t_0) = -i\,\theta(t_e - t_0)(\psi(\boldsymbol{x}_e, t_e)\,\psi^{\dagger}(\boldsymbol{x}_0, t_0) - \psi^{\dagger}(\boldsymbol{x}_0, t_0)\psi(\boldsymbol{x}_e, t_e))\phi_0 \quad (25)$$

where $\theta$ is the time ordering step function and $\psi$ respective $\psi^{\dagger}$ represent quantum field operators in the interaction representation. So, for example the creation field operator is normalized in a box V and reads

$$\psi^{\dagger}(\boldsymbol{x}, t) = \frac{1}{\sqrt{\mathrm{V}}} \sum_{\boldsymbol{k}} \widetilde{nt}^{\dagger}_{m_{tr},\boldsymbol{k}}(0)\, e^{-i\boldsymbol{k}\cdot\boldsymbol{x} + i\nu_{\boldsymbol{k}} t}, \quad (26)$$

where by $\widetilde{nt}^{\dagger}_{m_{tr},\boldsymbol{k}}(0)$ denotes a modified creation operator without annotation of the spatial position $x \in \mathrm{V}$ and the frequency $\nu_{\boldsymbol{k}}$.

The interaction Hamiltonian is defined as

$$H_{int}(t) = \int \psi^{\dagger}(\boldsymbol{x}, t)\, \psi(\boldsymbol{x}, t)\, V(\boldsymbol{x}, t)\, d^3x, \quad (27)$$

here $V(\boldsymbol{x}, t)$ represents a radial potential for small molecules, e.g. the van der Waals potential

$$V_{vdW}(r) = \frac{C_1 e^{-br}}{r} - \frac{C_6}{r^6}, \text{ where } C_1 \text{and } C_6 \text{ are constants,} \quad (28)$$

and the parameter $b$ represents the inverse of the equilibrium distance $r_{eqm}$ at which the potential becomes minimal. A typical value for this distance for small-size transmitters is $r_{eqm} \approx 0.3$ nm. The Lenard-Jones potential is given by

$$V_{LJ}(r) = \frac{A_6}{r^6} - \frac{A_{12}}{r^{12}}, \text{ with the two constants } A_6 \text{ and } A_{12}. \quad (29)$$

Both potentials have as well as a repulsive and an attractive part (dispersion binding potential). The repulsive forces typically exert their influence in a distance, which is smaller than ca. $\frac{1}{3}\, r_{eqm}$, which in our field of application means ca. 0.1 nm. The implication that repulsive or attractive forces may exert their mutual influences cause the effect that we may observe elastic scattering or inelastic scattering. In the last mentioned case, the momentum of the impinging molecule is strong enough, so it will not join to the other molecule but continue his now deviated path. However, for reasons of consistency of our quantum base objective we will not go into such molecular details and continue with our

previous executions. (31)

The Green´s function of a free particle is given by

$$G_0(\boldsymbol{x}_e, t_e;\, \boldsymbol{x}_0, t_0) = -i\theta(t_e - t_0)\, \tfrac{1}{\mathrm{V}} \textstyle\sum_{\boldsymbol{k}} e^{i\boldsymbol{k}\cdot(x_e - x_0) - i\nu_k (t_e - t_0)}. \quad (30)$$

In the following, we finally calculate the spatial perturbation expansion of the scattered fields until the third order. Hereby, we will in each order begin with the time dependent field and then transform it in a corresponding spatial and time representation. Both kinds of fields are also defined in the interaction representation,

If a molecule is scattered once by a potential $V$ then we can represent this process by the following field of first order

$$\Phi^{(1)}(t) = \phi(0) + \tfrac{1}{\hbar}\textstyle\int_0^t \int \psi^\dagger(\boldsymbol{x}, \tau)\, \psi(\boldsymbol{x}, \tau)\; V(\boldsymbol{x}, \tau)\, \phi(0)\, d\tau\, d^3\boldsymbol{x}.$$

The integration is carried out over all locations and times (path integral). Hereby, we assume that the initial state is settled by $\phi(0) = \psi^\dagger(\boldsymbol{x}_0, t_0)\, \phi_0$. Such time dependent fields usually are applied to construct non-relativistic Feynman graphs [16]. However, for reasons of brevity we refrain from the description of such graphs in this article.

The calculation of the following expectation value with respect of $\Phi^{(1)}(t)$ provides us with the path of a molecule, which is scattered once at location $(\boldsymbol{x}, t)$ and delivers to us the searched Green´s function

$$\langle \phi_0 | \psi(\boldsymbol{x}_e, t_e) | \Phi^{(1)}(t) \rangle = iG_0(\boldsymbol{x}_e, t_e;\, \boldsymbol{x}_0, t_0) + \quad (32)$$

$$\tfrac{i}{\hbar}\textstyle\int_0^t \int G_0(\boldsymbol{x}_e, t_e;\, \boldsymbol{x}, \tau)\, V(\boldsymbol{x}, \tau)\, G_0(\boldsymbol{x}, \tau;\, \boldsymbol{x}_0, t_0)\, d\tau\, d^3\boldsymbol{x} = iG_0(\boldsymbol{x}_e, t_e;\, \boldsymbol{x}_0, t_0) + G^{(1)}(\boldsymbol{x}_e, t_e;\, \boldsymbol{x}_0, t_0).$$

Here, for reasons of generality the limits on the spatial integral have been expressed by $\pm\infty$. In a practical case these two limits are finite and are established by the applied potential. The second expression $G^{(1)}(\boldsymbol{x}_e, t_e;\, \boldsymbol{x}_0, t_0)$ describes a particle which is scattered once at the potential $V(\boldsymbol{x}, \tau)$.

In the next step, we calculate the second term of the perturbation approach. Here, the time dependent field of double scattering is given by

$$\Phi^{(2)}(t) = \phi(0) + \frac{1}{\hbar}\int_0^t \int \psi^\dagger(\boldsymbol{x}_1, \tau_1)\, G_0(\boldsymbol{x}_1, \tau_1;\, \boldsymbol{x}_0, t_0)\, V(\boldsymbol{x}_1, \tau_1)\, \phi_0\, d^3\boldsymbol{x}_1\, d\tau_1 +$$

$$\left(-\frac{i}{\hbar}\right)^2 \int_0^t \int_0^{\tau_2} \int\int \psi^\dagger(\boldsymbol{x}_2, \tau_2)\, G_0(\boldsymbol{x}_2, \tau_2;\, \boldsymbol{x}_1, \tau_1)\, V(\boldsymbol{x}_2, \tau_2)\, G_0(\boldsymbol{x}_1, \tau_1;\, \boldsymbol{x}_0, t_0)\, V(\boldsymbol{x}_1, \tau_1)$$

$$\phi_0\, d^3\boldsymbol{x}_1 d\tau_1 d^3\boldsymbol{x}_2 d\tau_2. \quad (33)$$

The calculation of the corresponding expectation value is carried out as follows

$$\langle \phi_0 | \psi(\boldsymbol{x}_e, t_e) | \Phi^{(2)}(t) \rangle = iG_0(\boldsymbol{x}_e, t_e;\, \boldsymbol{x}_0, t_0) + \quad (34)$$

$$\frac{i}{\hbar}\int_0^t \int G_0(\boldsymbol{x}_e, \tau_e;\, \boldsymbol{x}_1, \tau_1)\, V(\boldsymbol{x}_1, \tau_1)\, G_0(\boldsymbol{x}_1, \tau_1;\, \boldsymbol{x}_0, t_0)\, d\tau_1\, d^3\boldsymbol{x}_1 +$$

$$\left(-\frac{i}{\hbar}\right)^2 i \int_0^t d\tau_2 \int_0^{\tau_2} \iint G_0(\boldsymbol{x}_e, t_e;\, \boldsymbol{x}_2, \tau_2)\, V(\boldsymbol{x}_2, \tau_2)\, G_0(\boldsymbol{x}_2, \tau_2;\, \boldsymbol{x}_1, \tau_1) V(\boldsymbol{x}_1, \tau_1) \cdot$$

$$G_0(\boldsymbol{x}_1, t_1;\, \boldsymbol{x}_0, t_0)\, d^3\boldsymbol{x}_1 d\tau_1 d^3\boldsymbol{x}_2.$$

The last term of the expression (34) defines the Green´s function for double scattering $G^{(2)}(\boldsymbol{x}_e, t_e;\, \boldsymbol{x}_0, t_0)$.

If a molecule may be scattered triply then we have to calculate the following field of third order

$$\Phi^{(3)}(t) = \phi(0) + \tfrac{1}{i\hbar}\textstyle\int_0^t \int \psi^\dagger(\boldsymbol{x}_1, \tau_1)\, iG_0(\boldsymbol{x}_1, \tau_1;\, \boldsymbol{x}_0, t_0)\, V(\boldsymbol{x}_1, \tau_1)\; d\boldsymbol{x}_1 d\tau_1 + \quad (35)$$

$$\left(-\frac{i}{\hbar}\right)^2 \int_0^t d\tau_2 \int_0^{\tau_2} \iint \psi^\dagger(\boldsymbol{x}_2, \tau_2)\, G_0(\boldsymbol{x}_2, \tau_2;\, \boldsymbol{x}_1, t_1) V(\boldsymbol{x}_2, \tau_2) \cdot\; G_0(\boldsymbol{x}_1, \tau_1;\, \boldsymbol{x}_0, t_0)\, V(\boldsymbol{x}_1, \tau_1)\, d\boldsymbol{x}_1 d\tau_1 d\boldsymbol{x}_2 +$$

$$\left(-\frac{i}{\hbar}\right)^3 \int_0^t d\tau_3 \int_0^{\tau_3} d\tau_2 \int_0^{\tau_2} \iiint \psi^\dagger(\boldsymbol{x}_3, \tau_3)\, G_0(\boldsymbol{x}_3, \tau_3;\, \boldsymbol{x}_2, \tau_2)\, V(\boldsymbol{x}_3, \tau_3) \cdot$$

$$G_0(\boldsymbol{x}_2, \tau_2;\, \boldsymbol{x}_1, \tau_1)\, V(\boldsymbol{x}_2, \tau_2)\, G_0(\boldsymbol{x}_1, \tau_1;\, \boldsymbol{x}_0, t_0)\, V(\boldsymbol{x}_1, \tau_1)\; d\boldsymbol{x}_1 d\tau_1 d\boldsymbol{x}_2 d\boldsymbol{x}_3.$$

The calculation of the corresponding expectation value is carried out as before

$$\langle \phi_0 | \psi(\boldsymbol{x}_e, t_e) | \Phi^{(3)}(t) \rangle = iG_0(\boldsymbol{x}_e, t_e;\, \boldsymbol{x}_0, t_0) + \quad (36)$$

$$\frac{i}{\hbar}\int_0^t \int G_0\left(\boldsymbol{x}_e, t_e;\, \boldsymbol{x}_1, \tau_1\right) V\left(\boldsymbol{x}_1, \tau_1\right) G_0\left(\boldsymbol{x}_1, \tau_1;\, \boldsymbol{x}_0, t_0\right) d\boldsymbol{x}_1 d\tau_1 \;+$$

$$\left(\frac{1}{i\hbar}\right)^2 \int_0^t \int_0^{\tau_2} \iint iG_0\left(\boldsymbol{x}_e, t_e;\, \boldsymbol{x}_2, \tau_2\right) \psi^{\dagger}\left(\boldsymbol{x}_2, \tau_2\right) iG_0\left(\boldsymbol{x}_2, \tau_2;\, \boldsymbol{x}_1, t_1\right) V\left(\boldsymbol{x}_2, \tau_2\right) \cdot$$

$$iG_0\left(\boldsymbol{x}_1, \tau_1;\, \boldsymbol{x}_0, t_0\right) V\left(\boldsymbol{x}_1, \tau_1\right) d\tau_1 d\boldsymbol{x}_1 d\boldsymbol{x}_2 d\tau_2 +$$

$$\left(-\frac{i}{\hbar}\right)^3 \int_0^t \int_0^{\tau_3} \int_0^{\tau_2} \iiint G_0\left(\boldsymbol{x}_e, t_e;\, \boldsymbol{x}_3, \tau_3\right) G_0\left(\boldsymbol{x}_3, \tau_3;\, \boldsymbol{x}_2, \tau_2\right) V\left(\boldsymbol{x}_3, \tau_3\right) \cdot$$

$$G_0\left(\boldsymbol{x}_2, \tau_2;\, \boldsymbol{x}_1, \tau_1\right) V\left(\boldsymbol{x}_2, \tau_2\right) G_0\left(\boldsymbol{x}_1, \tau_1;\, \boldsymbol{x}_0, t_0\right) V\left(\boldsymbol{x}_1, \tau_1\right) d\boldsymbol{x}_1 d\tau_1 d\boldsymbol{x}_2 d\tau_2 d\boldsymbol{x}_3 d\tau_3.$$

Here, we tacitly assumed the time ordering restriction $t < \tau_3 < \tau_2 < \tau_1 < \tau_0$. Equivalent restrictions are also valid in the two previous calculations of order 1 and 2. The last term of expression (3.32) defines the Green´s function of third order, which describe the triple scattering of a particle $G^{(3)}(\boldsymbol{x}_e, t_e;\, \boldsymbol{x}_0, t_0)$.

In this subsection we are focused to scattering processes therefore we are mainly concerned with the corresponding Green´s functions of the three different orders. The total amplitude for motion of a transmitter molecule from $(\boldsymbol{x}_0, t_0)$ to $(\boldsymbol{x}_e, t_e)$ with any number of scattering is given by $G_0 + G^{(1)} + G^{(2)} + G^{(3)} + \cdots + G^{(n)}$.

So far, we have introduced the Green´s function in the more accustomed $(\boldsymbol{x}, t)$- representation. However, it can also be defined in the $(\boldsymbol{k}, t)$- representation, which corresponds to the particle number representation of QFT. Here, the Green´s function of a free particle is denoted by

$G_{\boldsymbol{k}}(t) = -ie^{-iv_{\boldsymbol{k}}t}$, $t \geq 0$, otherwise 0.

The general Green´s function is defined by

$$G_{\boldsymbol{k}_e,\boldsymbol{k}_0}(t_e, t_0) = -i\,\theta(t_e - t_0)\,\langle\phi|\,\widetilde{nt}_{m_{tr},\boldsymbol{k}_e}(t_e)\,\widetilde{nt}^{\dagger}_{m_{tr},\boldsymbol{k}_0}(t_0)|\phi\rangle. \quad (37)$$

Thus, for example the twofold scattering in this space is expressed by

$$G_{\boldsymbol{k}_e,\boldsymbol{k}_2,\boldsymbol{k}_1,\boldsymbol{k}_0}(t_e, t_2; t_1, t_0) = i^3 G_{\boldsymbol{k}_e,\boldsymbol{k}_2}(t_e, t_2)\, G_{\boldsymbol{k}_2,\boldsymbol{k}_1}(t_2, t_1)\, G_{\boldsymbol{k}_1,\boldsymbol{k}_0}(t_1, t_0). \quad (38)$$

## Approach 2: Quantum Diffusion

Our second approach describes the transmission as an elementary quantum diffusion process, meaning that we e.g. exclude in our approximation the description of a diffuse modulatory system [4]. We begin our description with the representation of a one-particle state and then extend this approach to an n-particle system. The one-particle field operator is normalized in a cube of volume $V$ and is given by a plane wave expansion

$$\psi(\boldsymbol{x}, t) = \frac{1}{\sqrt{V}} \sum_{\boldsymbol{k}} \widetilde{nt}_{m_{tr},\boldsymbol{k}}(t)\, e^{i\boldsymbol{k}\cdot\boldsymbol{x}}\,. \quad (39)$$

Thus, the respective density of a particular neurotransmitter reads

$$\rho(\boldsymbol{x}, t) = \psi^{\dagger}(\boldsymbol{x}, t)\psi(\boldsymbol{x}, t) = \frac{1}{V}\sum_{\boldsymbol{k}} \widetilde{nt}^{\dagger}_{m_{tr},\boldsymbol{k}}(t)\, e^{-i\boldsymbol{k}\cdot\boldsymbol{x}} \sum_{\boldsymbol{k}'} \widetilde{nt}_{m_{tr},\boldsymbol{k}'}(t)\, e^{i\boldsymbol{k}'\cdot\boldsymbol{x}}. \quad (40)$$

The corresponding particular molecular current density is

$$\boldsymbol{j}(\boldsymbol{x}, t) = -D\,\nabla_{\boldsymbol{x}}\,\rho(\boldsymbol{x}, t), \quad (41)$$

where $D = \frac{\langle x^2\rangle}{2t} = \frac{l^2}{2t} = \frac{l}{2}\,\langle \mathrm{v}\rangle$ is the diffusion coefficient [10]. It is given in terms of the mean free-path $l$ and the mean velocity $\langle \mathrm{v}\rangle$. Typical values are $D \approx \frac{1}{2}10^{-8}\,cm^2/s$, $l \approx 10^{-8}cm$ and the time $\tau$ between two scattering processes is $\tau \approx 10^{-8}s$. By the use of the mobility $\mu = \frac{\tau}{m}$, where $m$ is the particle mass, we can define a temperature-dependent diffusion coefficient $D = \mu k_B T$, with the Boltzmann constant $k_B$ and the temperature $T$.

The divergence of the current defined by equation (39)) reads

$$\nabla_{\boldsymbol{x}} \cdot \boldsymbol{j}(\boldsymbol{x}, t) = -D\,\Delta_{\boldsymbol{x}}\,\rho(\boldsymbol{x}, t) = \quad (42)$$

$$\frac{\mathrm{D}}{\mathrm{V}}\left[\sum_{\boldsymbol{k},\boldsymbol{k}'}(\boldsymbol{k}^2 + \boldsymbol{k}'^2)\,\widetilde{nt}^{\dagger}_{m_{tr},\boldsymbol{k}}(t)\,\widetilde{nt}_{m_{tr},\boldsymbol{k}'}(t) e^{-i(\boldsymbol{k}-\boldsymbol{k}')\cdot\boldsymbol{x}}\right].$$

The diffusion of the concentration of neurotransmitters through the synaptic cleft is subjected to the continuity equation

$$\frac{\partial}{\partial t}\rho(\boldsymbol{x}, t) = -\nabla_{\boldsymbol{x}} \cdot \boldsymbol{j}(\boldsymbol{x}, t) = \mathrm{D}\,\Delta_{\boldsymbol{x}}\,\rho(\boldsymbol{x}, t). \quad (43)$$

The written – out version of this conservation law in the representation of creation and respectively destruction operators is

$$\frac{\partial}{\partial t}\left[\frac{1}{V}\sum_{\boldsymbol{k},\boldsymbol{k}'}\left(\widetilde{nt}^{\dagger}_{m_{tr},\boldsymbol{k}}(t)\,\widetilde{nt}_{m_{tr},\boldsymbol{k}'}(t)\right) e^{-i(\boldsymbol{k}-\boldsymbol{k}')\cdot\boldsymbol{x}}\right] = \quad (44)$$

$$D\left[\frac{1}{V}\sum_{\boldsymbol{k},\boldsymbol{k}'}(\boldsymbol{k}^2 + \boldsymbol{k}'^2)\,\widetilde{nt}^{\dagger}_{m_{tr},\boldsymbol{k}}(t)\,\widetilde{nt}_{m_{tr},\boldsymbol{k}'}(t) e^{-i(\boldsymbol{k}-\boldsymbol{k}')\cdot\boldsymbol{x}}\right].$$

The integral form of the continuity equation given by expression (3.36) reads

$$\frac{d}{dt}\int_V \rho(\boldsymbol{x}, t) d^3\boldsymbol{x} = -\int_{\partial V} \boldsymbol{j}\cdot\boldsymbol{n}\, da = -\int_V \nabla_{\boldsymbol{x}}\cdot\boldsymbol{j}\, d^3\boldsymbol{x}, \quad (45)$$

where $V$ is the normalizing volume, $\boldsymbol{n}$ denotes the unit surface normal, $da$ represents the surface element, and the last integral invokes the Gauss´s theorem. The number

operator $N_V$, which results from the integral over the volume $V$ of the corresponding particle density

$$N_V(t) = \int_V \rho(\boldsymbol{x},t)\, d^3\boldsymbol{x} = \tag{46}$$

$$\sum_{\boldsymbol{k}} \widetilde{nt}^{\dagger}_{m_{tr},\boldsymbol{k}}(t)\, \widetilde{nt}_{m_{tr},\boldsymbol{k}}(t) = \sum_{\boldsymbol{k}} N_{\boldsymbol{k}}(t) = \rho_{\boldsymbol{k}}(t).$$

Only the integration over the whole space (continuum normalization) would yield a time-independent total number operator [26]

$$N = \int_{-\infty}^{+\infty} \rho(\boldsymbol{x},t)\, d^3\boldsymbol{x} = \sum_{\boldsymbol{k}} \widetilde{nt}^{\dagger}_{m_{tr},\boldsymbol{k}}(0)\, \widetilde{nt}_{m_{tr},\boldsymbol{k}}(0). \tag{47}$$

After this remark we come back to the previous accomplishment with box normalized field operators and calculate the expectation value of the local number operator $N_{\boldsymbol{k}}(t)$

$$\langle\phi_{\{n\}}|\, N_{\boldsymbol{k}}(t)|\phi_{\{n\}}\rangle = \langle\phi_{\{n\}}|\, \widetilde{nt}^{\dagger}_{m_{tr},\boldsymbol{k}}(t)\, \widetilde{nt}_{m_{tr},\boldsymbol{k}}(t)|\phi_{\{n\}}\rangle = \langle n_{\boldsymbol{k}}\rangle, \tag{48}$$

which denotes the average number of particles of state $\boldsymbol{k}$ at time $t$. Even more, we can say that this expression can be interpreted as the probability to find a single neurotransmitter in quantum state $\boldsymbol{k}$ at time $t$, provided the following two conditions are fulfilled. At first, the function $\phi_{\{n\}}$ which is not time-dependent and represents the simultaneous eigenstates of $N_{\boldsymbol{k}_1}, N_{\boldsymbol{k}_2},\ldots, N_{\boldsymbol{k}_n}$ by the appropriate number of creation operators

$$\phi_{\{n\}} = \frac{1}{\left(n_{\boldsymbol{k}_1}! n_{\boldsymbol{k}_2}! \ldots n_{\boldsymbol{k}_n}!\right)^{1/2}} \left(\widetilde{nt}^{\dagger}_{m_{tr},\boldsymbol{k}_1}\right)^{n_{\boldsymbol{k}_1}} \left(\widetilde{nt}^{\dagger}_{m_{tr},\boldsymbol{k}_2}\right)^{n_{\boldsymbol{k}_2}} \ldots \left(\widetilde{nt}^{\dagger}_{m_{tr},\boldsymbol{k}_n}\right)^{n_{\boldsymbol{k}_n}} \phi_0 \tag{49}$$

$$= |n_{\boldsymbol{k}_1}, n_{\boldsymbol{k}_2}, \ldots., n_{\boldsymbol{k}_n}>$$

is normalized. At second, the following condition must be fulfilled

$$\frac{1}{N_{tot}} \sum_{\boldsymbol{k}=0} \langle\phi_{\{n\}}|\, \widetilde{nt}^{\dagger}_{m_{tr},\boldsymbol{k}}(t)\, \widetilde{nt}_{m_{tr},\boldsymbol{k}}(t)\, |\phi_{\{n\}}\rangle = 1, \text{ where } N_{tot} = \sum_{k=0} \langle n_{\boldsymbol{k}}\rangle. \tag{50}$$

Both conditions are fulfilled; therefore, we consider each normalized matrix element

$$\frac{1}{N_{tot}} \langle\phi_{\{n\}}|\, \widetilde{nt}^{\dagger}_{m_{tr},\boldsymbol{k}}(t)\, \widetilde{nt}_{m_{tr},\boldsymbol{k}}(t)\, |\phi_{\{n\}}\rangle = \frac{1}{N_{tot}} \langle\phi_{\{n\}}|\, \rho_{\boldsymbol{k}}(t)|\phi_{\{n\}}\rangle,\ \boldsymbol{k} = 0,1,2,\ldots \tag{51}$$

as an element of the time-dependent, diagonal, density matrix $\rho(\boldsymbol{k},t)$ in the particle representation. The equation (49) corresponds to the normalization of this matrix, trace $\rho(\boldsymbol{k},t) = 1$.

The expectation value of non-diagonal elements of matrix $\rho(\boldsymbol{k},t)$ is expressed by

$$\langle\phi_{\{n\}}|\, \widetilde{nt}^{\dagger}_{m_{tr},\boldsymbol{k}}(t)\, \widetilde{nt}_{m_{tr},\boldsymbol{k}}(t)\, |\phi_{\{m\}}\rangle = \langle n_{\boldsymbol{k}}\rangle \prod_{\boldsymbol{k}} \delta_{n_{\boldsymbol{k}} m_{\boldsymbol{k}}}. \tag{52}$$

Expectation values of a pair of different creation operators, which may occur in interaction Hamiltonians

$$\langle\phi_{\{n\}}|\, \widetilde{nt}^{\dagger}_{m_{tr},\boldsymbol{k}_i}(t)\, \widetilde{nt}_{m_{tr},\boldsymbol{k}_j}(t)|\phi_{\{n\}}\rangle = \delta_{n_{\boldsymbol{k}_i} n_{\boldsymbol{k}_j}}, \text{ if } \boldsymbol{k}_j = \boldsymbol{k}_1, \ldots, \boldsymbol{k}_n; \text{ otherwise } 0. \tag{53}$$

In the next step we carry out the calculation of the quantum information

$inf(\rho_{\boldsymbol{k}}(0)) = -\mathrm{trace}(\rho(\boldsymbol{k},0)\ln\rho(\boldsymbol{k},0))$ at time $t = 0$. We evaluate $inf(\rho(\boldsymbol{k},0))$ at $t = 0$ because we are interested in energetic steady-states which correspond to the Hamiltonian $H = \sum_k H_{\boldsymbol{k}} = \sum_k \hbar\omega_{\boldsymbol{k}} N_{\boldsymbol{k}}$. This Hamiltonian represent the energy of a field of non-interacting spinless particles. It is obvious, that we get with this calculation without any remarkable, additional effort also the final expression for the density matrix for $N_V(0) = \sum_k N_{\boldsymbol{k}}$. We accomplish the energy-based evaluation the density matrix by the aid of the following general formula [17]

$$\rho_{\boldsymbol{k}}(0) = e^{\lambda - \lambda_1 \mathrm{H}}, \tag{54}$$

where the two parameters $\lambda$ and $\lambda_1$ are Lagrange parameters. The $\lambda$ parameter is determined by

$e^{\lambda} = Z$ and Z defines the partition function

$$Z = \mathrm{trace}\left(e^{-\beta H}\right) = \sum_{\boldsymbol{k}} e^{-\beta E_{\boldsymbol{k}}} = \sum_{\boldsymbol{k}} e^{-\beta\hbar\omega_{\boldsymbol{k}} n_{\boldsymbol{k}}} = \sum_{\boldsymbol{k}} e^{(-\beta\hbar\omega_{\boldsymbol{k}})^{n_{\boldsymbol{k}}}}. \tag{55}$$

The second parameter is $\lambda_1 = \beta = 1/k_B T$.

The calculation of $inf(\rho_{\boldsymbol{k}}(0))$ is carried out by the application of equation (A)

$$inf((\rho(\boldsymbol{k},0)) = e^{-\lambda}\left[\lambda\, \mathrm{trace}\left(e^{-\lambda_1 \mathrm{H}}\right) + \lambda_1 \mathrm{trace}\left(e^{-\lambda_1 \mathrm{H}}\right)\mathrm{H}\right] = \tag{56}$$

$$e^{-\lambda}[\lambda \sum_{\boldsymbol{k}=0}^{\infty} \exp\{-\lambda_1 \hbar\omega_{\boldsymbol{k}})^{n_{\boldsymbol{k}}}] + \lambda_1 \frac{\sum_{\boldsymbol{k}=0}^{\infty} \exp\{-\lambda_1 \hbar\omega_{\boldsymbol{k}})^{n_{\boldsymbol{k}}}\, \hbar\omega_{\boldsymbol{k}} n_{\boldsymbol{k}}}{\sum_{\boldsymbol{k}=0}^{\infty} \exp\{-\lambda_1 \hbar\omega_{\boldsymbol{k}})^{n_{\boldsymbol{k}}}}.$$

This expression can be cast in a simplified form if we insert the definitions of the two Lagrange parameters

$$inf((\rho(\boldsymbol{k},0)) = \ln\left(1 - \sum_{\boldsymbol{k}} e^{(-\beta\hbar\omega_{\boldsymbol{k}})^{n_{\boldsymbol{k}}}}\right) + \beta \frac{\sum_{\boldsymbol{k}=0}^{\infty} \exp\{-\beta\hbar\omega_{\boldsymbol{k}})^{n_{\boldsymbol{k}}}\, \hbar\omega_{\boldsymbol{k}} n_{\boldsymbol{k}}}{\sum_{\boldsymbol{k}=0}^{\infty} \exp\{-\beta\hbar\omega_{\boldsymbol{k}})^{n_{\boldsymbol{k}}}} \tag{57}$$

This result can be more simpler reproduced (except the factor $k_B$) if we calculate the entropy S which is defined in

thermodynamics by the formula

$$S = k_B \left(\ln Z - \beta \frac{\partial}{\partial \beta} \ln Z\right). \tag{58}$$

This conformity is not accidental but reveals the close connections between quantum statistics and classical physical statistics. Therefore, $inf(\rho(\boldsymbol{k},0))$ is also called information entropy.

The expression (57) is equivalent to the corresponding expression for a quantum oscillator if we assume that the frequencies are not $\boldsymbol{k}$-dependent but all are equal to a mean frequency $\omega_{\boldsymbol{k}} = \bar{\omega}$, then we get the result

$$\overline{inf((\rho(\boldsymbol{k},0))} = -\ln\left(1 - e^{-\beta\hbar\bar{\omega}}\right) + \frac{\beta\hbar\bar{\omega}}{e^{\beta\hbar\bar{\omega}-1}}. \tag{59}$$

The conservation law (43) in integral form is given by

$$\frac{\partial}{\partial t}\rho_{\boldsymbol{k}}(t) = \frac{\partial}{\partial t} \sum_{\boldsymbol{k}} \widetilde{nt}^{\dagger}_{m_{tr},\boldsymbol{k}}(t)\, \widetilde{nt}_{m_{tr},\boldsymbol{k}}(t) = \tag{60}$$

$$2\mathrm{D}\big[\sum_{\boldsymbol{k}} \boldsymbol{k}^2\, \widetilde{nt}^{\dagger}_{m_{tr},\boldsymbol{k}}(t)\, \widetilde{nt}_{m_{tr},\boldsymbol{k}}(t)\big],$$

hereby each particular term possesses the solution

$$\widetilde{nt}^{\dagger}_{m_{tr},\boldsymbol{k}}(t)\, \widetilde{nt}_{m_{tr},\boldsymbol{k}}(t) = 2D \int_0^t \boldsymbol{k}^2\, \widetilde{nt}^{\dagger}_{m_{tr},\boldsymbol{k}}(\tau)\, \widetilde{nt}_{m_{tr},\boldsymbol{k}}(\tau)\, d\tau + \widetilde{nt}^{\dagger}_{m_{tr},\boldsymbol{k}}(0)\, \widetilde{nt}_{m_{tr},\boldsymbol{k}}(0). \tag{61}$$

We continue the description of the diffusion process by passing over to the n-particles states

$$\psi^{\dagger}(\boldsymbol{x}_n, \boldsymbol{x}_{n-1}, \ldots, \boldsymbol{x}_1; t) = \frac{1}{\sqrt{n!}} \psi^{\dagger}(\boldsymbol{x}_n, t)\psi^{\dagger}(\boldsymbol{x}_{n-1}, t) \ldots \psi^{\dagger}(\boldsymbol{x}_1, t) = \tag{62}$$

$$\frac{1}{\mathrm{V}^{n/2}} \frac{1}{\sqrt{n!}} \left(\sum\nolimits_{\boldsymbol{k}_n} \widetilde{nt}^{\dagger}_{m_{tr},\boldsymbol{k}_n}(t)\, e^{-i\boldsymbol{k}_n \cdot \boldsymbol{x}_n}\right) \ldots \left(\sum\nolimits_{\boldsymbol{k}_1} \widetilde{nt}^{\dagger}_{m_{tr},\boldsymbol{k}_1}(t)\, e^{-i\boldsymbol{k}_1 \cdot \boldsymbol{x}_1}\right)$$

describes the creation of $n$ equal particles at different positions $\boldsymbol{x}_n, \boldsymbol{x}_{n-1}, \ldots, \boldsymbol{x}_1$ at the time t.

The corresponding n-particle spatial density is expressed by

$$\rho_n(\{\boldsymbol{x}_j\}, t) = \tag{63}$$

$$\frac{1}{n!} \psi^{\dagger}(\boldsymbol{x}_n, t)\psi(\boldsymbol{x}_n, t)\psi^{\dagger}(\boldsymbol{x}_{n-1}, t)\psi(\boldsymbol{x}_{n-1}, t) \ldots \ldots \psi^{\dagger}(\boldsymbol{x}_1, t)\psi(\boldsymbol{x}_1, t) =$$

$$\frac{1}{n!}\rho(\boldsymbol{x}_n, t) \ldots \rho(\boldsymbol{x}_1, t),$$

where the reordering of the last line is permitted by our assumption that all field operators obey the Bose-Einstein statistics and therefore they commute under position exchange at the same time.

If we replace in expression (60) the field operators by their decomposition in plane waves then the n-particle density operator can be reformulated as follows

$$\rho_n(\{\boldsymbol{x}_j\}, t) = \tag{64}$$

$$\frac{1}{\mathrm{V}^{n/2}} \frac{1}{n!} \left(\sum\nolimits_{\boldsymbol{k}_n, \boldsymbol{k}_n'} \widetilde{nt}^{\dagger}_{m_{tr},\boldsymbol{k}_n}(t)\, \widetilde{nt}_{m_{tr},\boldsymbol{k}_n'}(t)\, e^{-i(\boldsymbol{k}_n - \boldsymbol{k}_n')\cdot \boldsymbol{x}_n}\right) \ldots$$

$$\left(\sum\nolimits_{\boldsymbol{k}_1, \boldsymbol{k}_1'} \widetilde{nt}^{\dagger}_{m_{tr},\boldsymbol{k}_1}(t)\, \widetilde{nt}_{m_{tr},\boldsymbol{k}_1'}(t)\, e^{-i(\boldsymbol{k}_1 - \boldsymbol{k}_1')\cdot \boldsymbol{x}_1}\right).$$

By integration of this density over $\{\boldsymbol{x}_j\}$ we obtain the n-particle density in $\boldsymbol{k}$-representation in direct analogy to equation (44)

$$\rho_n(\{\boldsymbol{k}_j\}, t) = \int_V \rho_{tot}(\{\boldsymbol{x}_j\}, t) d^3\{\boldsymbol{x}_j\} = \frac{1}{n!} \rho_{\boldsymbol{k}_n}(t) \ldots . \rho_{\boldsymbol{k}_1}(t), \tag{65}$$

where $\rho_{\boldsymbol{k}_n}$ denotes the density of the nth transmitter which is in state $\boldsymbol{k}_n$, $\rho_{\boldsymbol{k}_{n-1}}$ represent the density of particle which are in state $\boldsymbol{k}_{n-1}$, etc. Moreover, we anticipate that all transmitters are of identical type (sub-index $m_{tr}$ is fixed) because they are released from one vesicle, thus $n = 10^3$ to $10^4$.

After the calculations of $\rho_n$ in the $\boldsymbol{x}$-space and the $\boldsymbol{k}$-space we continue our execution by focusing to the evaluation of continuity equation for both just mentioned notations. The current density for $n$ particles in the configuration space is given by

$$\boldsymbol{j}_n(\{\boldsymbol{x}_j\}, t) = -\mathrm{D}\, \nabla_{\boldsymbol{x}}\, \rho_n(\{\boldsymbol{x}_j\}, t) = \tag{66}$$

$$-\mathrm{D} \frac{1}{\mathrm{V}^{n/2}} \frac{1}{n!} \Big[\left(\nabla_{\boldsymbol{x}}\, \psi^{\dagger}(\boldsymbol{x}_n, t)\right) \psi(\boldsymbol{x}_n, t)\, \psi^{\dagger}(\boldsymbol{x}_{n-1}, t) \ldots \psi^{\dagger}(\boldsymbol{x}_1, t)\psi(\boldsymbol{x}_1, t)$$

$$\ldots + \psi^{\dagger}(\boldsymbol{x}_n, t)\psi(\boldsymbol{x}_n, t)\psi^{\dagger}(\boldsymbol{x}_{n-1}, t) \ldots \psi^{\dagger}(\boldsymbol{x}_1, t) \left(\nabla_{\boldsymbol{x}} \psi(\boldsymbol{x}_1, t)\right)\Big].$$

The divergence of this current is denoted by

$$\nabla_x \cdot \boldsymbol{j}_n(\{\boldsymbol{x}_j\},t) = -D\Delta_x \boldsymbol{j}_n(\{\boldsymbol{x}_j\},t) = \tag{67}$$

$$D\frac{1}{V^{n/2}}\frac{1}{n!}\Big[\sum\nolimits_{\boldsymbol{k}_n,\boldsymbol{k}'_n}(\boldsymbol{k}_n^2+\boldsymbol{k}'^2_n)\,\widetilde{nt}^{\dagger}_{m_{tr},\boldsymbol{k}_n}\widetilde{nt}_{m_{tr},\boldsymbol{k}'_n}(t)\,e^{-i(\boldsymbol{k}_n-\boldsymbol{k}'_n)\cdot\boldsymbol{x}_n}\Big]$$

$$\big[\textstyle\sum_{\boldsymbol{k}_{n-1},\boldsymbol{k}'_{n-1}}\widetilde{nt}^{\dagger}_{m_{tr},\boldsymbol{k}_{n-1}}(t)\,\widetilde{nt}_{m_{tr},\boldsymbol{k}'_{n-1}}(t)\,e^{-i(\boldsymbol{k}_{n-1}-\boldsymbol{k}'_{n-1})\cdot\boldsymbol{x}_{n-1}}\big]\dots$$

$$\big[\textstyle\sum_{\boldsymbol{k}_1,\boldsymbol{k}'_1}\widetilde{nt}^{\dagger}_{m_{tr},\boldsymbol{k}_1}(t)\,\widetilde{nt}_{m_{tr},\boldsymbol{k}'_1}(t)e^{-i(\boldsymbol{k}_1-\boldsymbol{k}'_1)\cdot\boldsymbol{x}_1}\big]+$$

$$\Big[\textstyle\sum_{\boldsymbol{k}_1,\boldsymbol{k}'_1}(\boldsymbol{k}_1^2+\boldsymbol{k}'^2_1)\,\widetilde{nt}^{\dagger}_{m_{tr},\boldsymbol{k}_1}\widetilde{nt}_{m_{tr},\boldsymbol{k}'_1}(t)\,e^{-i(\boldsymbol{k}_1-\boldsymbol{k}'_1)\cdot\boldsymbol{x}_1}\Big]\dots$$

$$\big[\textstyle\sum_{\boldsymbol{k}_n,\boldsymbol{k}'_n}\widetilde{nt}^{\dagger}_{m_{tr},\boldsymbol{k}_n}(t)\,\widetilde{nt}_{m_{tr},\boldsymbol{k}'_n}(t)\,e^{-i(\boldsymbol{k}_n-\boldsymbol{k}'_n)\cdot\boldsymbol{x}_n}\big]\dots$$

$$\big[\textstyle\sum_{\boldsymbol{k}_2,\boldsymbol{k}'_2}\widetilde{nt}^{\dagger}_{m_{tr},\boldsymbol{k}_2}\widetilde{nt}_{m_{tr},\boldsymbol{k}'_2}(t)\,e^{-i(\boldsymbol{k}_2-\boldsymbol{k}'_2)\cdot\boldsymbol{x}_2}\big].$$

In the next step we integrate equation (66)

$$-D\int_V \Delta_x \boldsymbol{j}_{tot}(\{\boldsymbol{x}_j\},t)\,d^3\boldsymbol{x}_n\ \dots d^3\boldsymbol{x}_1 = \tag{68}$$

$$2D\frac{1}{n!}\big[\big(\textstyle\sum_{\boldsymbol{k}_n}\boldsymbol{k}_n^2\widetilde{nt}^{\dagger}_{m_{tr},\boldsymbol{k}_n}\widetilde{nt}_{m_{tr},\boldsymbol{k}_n}(t)\big)\,\rho_{\boldsymbol{k}_{n-1}}(t)\dots.\,\rho_{\boldsymbol{k}_1}(t)+$$

$$\big(\textstyle\sum_{\boldsymbol{k}_{n-1}}\boldsymbol{k}_{n-1}^2\widetilde{nt}^{\dagger}_{m_{tr},\boldsymbol{k}_{n-1}}\widetilde{nt}_{m_{tr},\boldsymbol{k}_{n-1}}(t)\big)\,\rho_{\boldsymbol{k}_n}(t)\,\rho_{\boldsymbol{k}_{n-2}}(t)\dots.\,\rho_{\boldsymbol{k}_1}(t)+$$

$$\big(\textstyle\sum_{\boldsymbol{k}_1}\boldsymbol{k}_1^2\widetilde{nt}^{\dagger}_{m_{tr},\boldsymbol{k}_1}\widetilde{nt}_{m_{tr},\boldsymbol{k}_1}(t)\big)\rho(\{\boldsymbol{k}_n\},t)\rho_{\boldsymbol{k}_{n-1}}(,t)\dots\rho_{\boldsymbol{k}_2}(t)\}\big)\big].$$

This rearrangement of the number operators $\widetilde{nt}^{\dagger}_{m_{tr},\boldsymbol{k}_i}\widetilde{nt}_{m_{tr},\boldsymbol{k}_i}$ is permitted since they all commute (simultaneous eigenstates). The conservation equation can be expressed as follows

$$\Big[\Big(\frac{\partial}{\partial t}\rho_{\boldsymbol{k}_n}(t)\Big)\,\rho_{\boldsymbol{k}_{n-1}}(t)\dots\ \rho_{\boldsymbol{k}_1}(t)+ \tag{69}$$

$$\Big(\frac{\partial}{\partial t}\rho_{\boldsymbol{k}_{n-1}}(t)\Big)\,\rho_{\boldsymbol{k}_n}(t)\,\rho_{\boldsymbol{k}_{n-2}}(t)\dots.\,\rho_{\boldsymbol{k}_1}(t)\dots+\rho_{\boldsymbol{k}_n}(t)\dots\Big(\frac{\partial}{\partial t}\rho_{\boldsymbol{k}_1}(t)\Big)\Big]$$

$$=2D\big[\big(\textstyle\sum_{\boldsymbol{k}_n}\boldsymbol{k}_n^2\widetilde{nt}^{\dagger}_{m_{tr},\boldsymbol{k}_n}(t)\,\widetilde{nt}_{m_{tr},\boldsymbol{k}'_n}(t)\big)\,\rho_{\boldsymbol{k}_{n-1}}(t)\dots.\,\rho_{\boldsymbol{k}_1}(t)+$$

$$\big(\textstyle\sum_{\boldsymbol{k}_{n-1}}\boldsymbol{k}_{n-1}^2\widetilde{nt}^{\dagger}_{m_{tr},\boldsymbol{k}_{n-1}}\widetilde{nt}_{m_{tr},\boldsymbol{k}_{n-1}}(t)\big)\,\rho_{\boldsymbol{k}_n}(t)\,\rho_{\boldsymbol{k}_{n-2}}(t)\dots.\,\rho_{\boldsymbol{k}_1}(t)+\dots$$

$$\big(\textstyle\sum_{\boldsymbol{k}_1}\boldsymbol{k}_1^2\,\widetilde{nt}^{\dagger}_{m_{tr},\boldsymbol{k}_1}\widetilde{nt}_{m_{tr},\boldsymbol{k}_1}(t)\big)\rho_{\boldsymbol{k}_{n-1}}(t)\rho_{\boldsymbol{k}_{n-1}}(t)\dots\rho_{\boldsymbol{k}_2}(t)\big].$$

A comparison of each corresponding term from the left and the right hand side of this continuity equation yields the solution as given above by equation (60).

Here, we point out that the conservation law is modified if during the diffusion process several neurotransmitters are eliminated (e.g. annihilation by particular enzymes). In our notation, we have to introduce an additional sink. The integral form of the modified continuity equation reads

$$\frac{d}{dt}N_V = \int_V \nabla_x\cdot\boldsymbol{j}_{loss}\,d^3\boldsymbol{x}_n\,d^3\boldsymbol{x}_{n-1} - \int_V \nabla_x\cdot\boldsymbol{j}_n\,d^3\boldsymbol{x}_n\dots d^3\boldsymbol{x}_1, \tag{70}$$

where $\boldsymbol{j}_{loss}$ declares the loss current and $\boldsymbol{j}_n$ comprises all molecules. For example, we assume for a better ease of understanding of equation (69 that only two neurotransmitters with vectors $\boldsymbol{k}_n$ and $\boldsymbol{k}_{n-1}$ are eliminated. Then the written–out expression of the violated conservation law is given by

$$\frac{\partial}{\partial t}\big[\rho_{\boldsymbol{k}_{n-2}}(t)\dots\ \rho_{\boldsymbol{k}_1}(t)\big] = \tag{71}$$

$$2D\big[\big(\textstyle\sum_{\boldsymbol{k}_{n-2}}\boldsymbol{k}_{n-2}^2\,\widetilde{nt}^{\dagger}_{m_{tr},\boldsymbol{k}_{n-2}}\widetilde{nt}_{m_{tr},\boldsymbol{k}_{n-2}}(t)\big)\,\rho_{\boldsymbol{k}_{n-3}}(t)\,\rho_{\boldsymbol{k}_{n-4}}(t)\dots.\,\rho_{\boldsymbol{k}_1}(t)+$$

$$\big(\textstyle\sum_{\boldsymbol{k}_{n-3}}\boldsymbol{k}_{n-3}^2\,\widetilde{nt}^{\dagger}_{m_{tr},\boldsymbol{k}_{n-3}}\widetilde{nt}_{m_{tr},\boldsymbol{k}_{n-3}}(t)\big)\,\rho_{\boldsymbol{k}_{n-2}}(t)\,\rho_{\boldsymbol{k}_{n-4}}(t)\dots.\,\rho_{\boldsymbol{k}_1}(t)+\dots$$

$$\big(\textstyle\sum_{\boldsymbol{k}_1}\boldsymbol{k}_1^2\,\widetilde{nt}^{\dagger}_{m_{tr},\boldsymbol{k}_1}\widetilde{nt}_{m_{tr},\boldsymbol{k}_1}(t)\big)\rho_{\boldsymbol{k}_{n-2}}(,t)\rho_{\boldsymbol{k}_{n-3}},t)\dots\rho_{\boldsymbol{k}_2}(t)\big].$$

# Approach 3: Probability Amplitude of an n-Particle System

The initial point to calculate the amplitude of an n-particle system $\Psi(\boldsymbol{x}_1,\boldsymbol{x}_2,\dots,\boldsymbol{x}_n;t)$ is the Schrödinger equation of n equivalent and not interacting particles which are subjected to a general potential $V(\boldsymbol{x})$:

$$i\hbar\frac{\partial}{\partial t}\Psi(\boldsymbol{x}_1,\boldsymbol{x}_2,\dots,\boldsymbol{x}_n;t)=H\phi, \tag{72}$$

where $H=\sum_{j=1}^{n}H_l=\sum_{l=1}^{n}\left[-\frac{\hbar^2}{2m}\Delta_{\boldsymbol{x}_l}+V(\boldsymbol{x}_l)\right]$ is the sum of one particle solutions. The potential is set as a drift potential which is characterized by a force $\boldsymbol{F}=\boldsymbol{v}_{drift}/\mu$, where $\mu$ is the mobility and the force operates in a fixed **x**-direction, $V(\boldsymbol{x})=-\boldsymbol{F}\cdot\boldsymbol{x}$.

The special solution Ψ of equation (72) is a product of the particular solutions

$$u_l(\boldsymbol{x},t)=u_l(\boldsymbol{x})\,e^{\frac{iE_lt}{\hbar}},\ \Psi(\boldsymbol{x}_1,\boldsymbol{x}_2,\dots,\boldsymbol{x}_n;t)=\prod_{l=1}^{n}u_l(\boldsymbol{x}_l,t). \tag{73}$$

These eigenfunctions form an orthonormal and complete set of the n-particle Schrödinger equation. The general solution of is a linear combination of such special solutions, [7]. However, in our context we are more interested how many particles are in the particular steady states of definite energy $u_l(\boldsymbol{x}_l)$. The corresponding occupation number $n_l$ denotes this. In other words, we are looking for a probability amplitude which is both a solution of the n-particle Schrödinger equation (72) and establish the relation of the occupation number $n_l$ of the energy level $E_l=\frac{(\hbar\boldsymbol{k}_l)^2}{2m}$ with a particular position $x_i, i=1,2,\dots,n$. Notice, that there exist no conflict with respect to the Heisenberg uncertainty relation between $\boldsymbol{k}_l$ and $\boldsymbol{x}_i$ because $+\boldsymbol{k}_l$ and $-\boldsymbol{k}_l$ contribute both to the same energy. The wanted relation is assigned by the following scalar product

$$\langle\boldsymbol{x}_1,\boldsymbol{x}_2,\dots,\boldsymbol{x}_n\,|n_1,n_2,\dots,n_N;t\rangle, \tag{74}$$

where *N* denotes the number of one-particle energy levels. We select the particular scalar product $\langle\boldsymbol{x}_1,\boldsymbol{x}_2,\boldsymbol{x}_3;t\,|n_1,n_2,n_3,n_4\rangle$ to explain in more details the expression (74). Moreover, we assume that the four individual energy levels ($N=4$) have the following multiplicity: $n_1=2, n_2=1, n_3=1, n_4=2$. Then this commitment yields the following formula for the scalar product

$$\langle\boldsymbol{x}_1,\boldsymbol{x}_2,\boldsymbol{x}_3|n_1,n_2,n_3,n_4;t\rangle=u_1(\boldsymbol{x}_1,t)u_1(\boldsymbol{x}_2,t)u_2(\boldsymbol{x}_3,t)+u_1(\boldsymbol{x}_2,t)u_1(\boldsymbol{x}_3,t)u_2(\boldsymbol{x}_1,t)+u_1(\boldsymbol{x}_3,t)u_2(\boldsymbol{x}_2,t)u_1(\boldsymbol{x}_1,t)+u_3(\boldsymbol{x}_1,t)u_4(\boldsymbol{x}_2,t)u_4(\boldsymbol{x}_3,t)+u_3(\boldsymbol{x}_2,t)u_4(\boldsymbol{x}_3,t)u_4(\boldsymbol{x}_1,t)+u_3(\boldsymbol{x}_3,t)u_4(\boldsymbol{x}_1,t)u_4(\boldsymbol{x}_2,t). \tag{75}$$

The six terms represent the permutation of the three arguments applied on two different series of the $u_l$ functions. The plus sign of the second series $u_3u_4u_4$ is typical for Bosons, where $\Psi(\boldsymbol{x}_1,\boldsymbol{x}_2,\dots,\boldsymbol{x}_n;t))$ is symmetric, while for Fermions is $\Psi(\boldsymbol{x}_1,\boldsymbol{x}_2,\dots,\boldsymbol{x}_n;t)$ is antisymmetric. In the last mentioned case, we have to set in each of these three last terms a minus sign in front. This sign change can be achieved by the use of the corresponding Slater determinant.

The general, normalized n-particle solution for Bosons is given by

$$\Psi(\boldsymbol{x}_1,\boldsymbol{x}_2,\dots,\boldsymbol{x}_n;t)=\frac{1}{\sqrt{n!}}\sum_{n_1,\dots,n_n=1}^{N}c(n_1,\dots,n_n)\,\langle\boldsymbol{x}_1,\boldsymbol{x}_2,\dots,\boldsymbol{x}_n|n_1,n_2,\dots,n_N;t\rangle, \tag{76}$$

where the sequence of the indices $n_1,\dots,n_n$ of each coefficient $\mathrm{c}(n_1,\dots,n_n)$ has to be interpreted in directly coincidence to the order of the spatial variables. The density must be normalized $\int|\Psi(\boldsymbol{x}_1,\boldsymbol{x}_2,\dots,\boldsymbol{x}_n;t)|^2d^3\boldsymbol{x}_1\dots d^3\boldsymbol{x}_n=1$ and it must also be invariant under the exchange of arguments. That is, the two following conditions have got to be fulfilled:

$$\frac{1}{n!}\sum_{n_1,\dots,n_n=1}^{N}|\mathrm{c}(n_1,\dots,n_n)|^2=1, \tag{77}$$

$$\mathrm{c}(\dots,n_i,\dots,n_j\ \dots)=+\mathrm{c}(\dots,n_j,\dots,n_i\ \dots). \tag{78}$$

For reasons of clarity we go back to our previous example, given by (74) in order to describe the corresponding function

$$\Psi(\boldsymbol{x}_1,\boldsymbol{x}_2,\boldsymbol{x}_3;t)=\frac{1}{\sqrt{3!}}\sum_{n_1,\dots,n_4=1}^{4}c(n_i,n_j,n_k)\,\langle\boldsymbol{x}_1,\boldsymbol{x}_2,\boldsymbol{x}_3;t\,|n_1,n_2,n_3,n_4\rangle \tag{79}$$

$$=\frac{1}{\sqrt{3!}}[\mathrm{c}(n_1=1,n_2=1,n_3=1)u_1(\boldsymbol{x}_1,t)u_1(\boldsymbol{x}_2,t)u_2(\boldsymbol{x}_3,t)+\mathrm{c}(n_1=2,n_2=1,n_3=1)$$
$$u_1(\boldsymbol{x}_2,t)u_1(\boldsymbol{x}_3,t)u_2(\boldsymbol{x}_1,t)+\mathrm{c}(n_1=1,n_2=2,n_3=1)\,u_1(\boldsymbol{x}_3,t)u_2(\boldsymbol{x}_2,t)u_1(\boldsymbol{x}_1,t)+$$
$$\mathrm{c}(n_1=3,n_2=4,n_3=4)\,u_3(\boldsymbol{x}_1,t)u_4(\boldsymbol{x}_2,t)u_4(\boldsymbol{x}_3,t)+\mathrm{c}(n_1=4,n_2=3,n_3=4)\times$$
$$u_3(\boldsymbol{x}_2,t)u_4(\boldsymbol{x}_3,t)u_4(\boldsymbol{x}_1,t)+\mathrm{c}(n_1=4,n_2=3,n_3=4)\,u_3(\boldsymbol{x}_3,t)u_4(\boldsymbol{x}_1,t)u_4(\boldsymbol{x}_2,t)].$$

This example amplitude Ψ reveals more energy quants ($N=4$) than positions ($n=3$), thus, only three occupation numbers can be indicated in each coefficient. This inequality is expressed by the notation $(n_i,n_j,n_k)\,\epsilon\,\{n_1,n_2,n_3,n_4\}$.

The calculation of the coefficients $c(n_1,\dots,n_n)$ can be done if we use (77), which demands the pairwise symmetrical exchange of the occupation numbers. That is, if we know one of these coefficients then we can calculate the remaining $n!-1$ coefficients. If we again consider the example amplitude (75), then we can evaluate the following probabilities for the given distribution of occupation numbers:

$$\frac{|c_1|^2}{6}=0.2,\frac{|c_2|^2}{6}=0.2,\frac{|c_3|^2}{6}=0.2,\frac{|c_4|^2}{6}=0.13,\frac{|c_5|^2}{6}=0.13,\frac{|c_6|^2}{6}=0.13. \tag{80}$$

Here we used the abbreviation $c_i$ $(i=1,\dots,6)$ for the six coefficients in (75).

### *4.5. Fifth Phase: Reception*

*Hamiltonian of the reception step*

Receivers are frequently transmitter-gated ion channels, which can differ from one another in two principal ways. First, channels are very selective to the type of released neurotransmitters. Second, channels are highly selective which ions they let pass across the postsynaptic membrane. Here, we bring into focus that we consider only a selected spectrum of receptors e.g. acetylcholine-gated cation channel and voltage−gated $Na^+$, respectively $Ca^{2+}$ channels. Thus, we presume that several (ionotropic) creation operators of receivers $rc^{\dagger}_{m_{tr},s,\boldsymbol{x}_{rc}}$ exist, where $m_{tr}$ specifies the type of the neurotransmitter which can bind to a receiver. For ease of understanding we consider the three states e.g. of an acetylcholine receptor. The three states of this receiver are denoted by *s* and are characterized as follows: *unoccupied and closed* (*s* = 1), *occupied and open* (*s* = 2), *occupied and closed* (*s* = 3). From the state *s* = 3 it goes back to state *s* = 1. The location of a receiver is marked by $\boldsymbol{x}_{rc}$. In addition, we assume that only the reception of two neurotransmitters can cause the transitions between the different receiver states. Since a receptor opens a corresponding channel, we define also a creator operator of an ion-channel $ch^{\dagger}_{tr,\boldsymbol{x}_{ch}}$ and respectively $ch_{tr,\boldsymbol{x}_{ch}}$. Both operators determine the impact of channels and are strongly connected to the receiver type and also model the inflow of cations like $Na^+$ and even describe the case of no flow through the postsynaptic plasma membrane. The position of the ion-channel is indicated by $\boldsymbol{x}_{ch}$.

To simplify the calculations of the equations of motion we introduce the following state flip and inversion operators:

$$\alpha^{\dagger}_{rc,1} = rc^{\dagger}_{m_{tr},2,\boldsymbol{x}_{rc}}\, rc_{m_{tr},1,\boldsymbol{x}_{rc}}\,, \tag{81}$$

$$\sigma_{rc,1} = rc^{\dagger}_{m_{tr},2,\boldsymbol{x}_{rc}}\, rc_{m_{tr},2,\boldsymbol{x}_{rc}} - rc^{\dagger}_{m_{tr},1,\boldsymbol{x}_{rc}}\, rc_{m_{tr},1,\boldsymbol{x}_{rc}}\,.$$

$$\alpha^{\dagger}_{rc,2} = rc^{\dagger}_{m_{tr},3,\boldsymbol{x}_{rc}}\, rc_{m_{tr},2,\boldsymbol{x}_{rc}}\,, \tag{82}$$

$$\sigma_{rc,2} = rc^{\dagger}_{m_{tr},3,\boldsymbol{x}_{rc}}\, rc_{m_{tr},3,\boldsymbol{x}_{rc}} - rc^{\dagger}_{m_{tr},2,\boldsymbol{x}_{rc}}\, rc_{m_{tr},2,\boldsymbol{x}_{rc}}\,.$$

$$\alpha^{\dagger}_{rc,3} = rc^{\dagger}_{m_{tr},1,\boldsymbol{x}_{rc}}\, rc_{m_{tr},3,\boldsymbol{x}_{rc}}\,, \tag{83}$$

$$\sigma_{rc,3} = rc^{\dagger}_{m_{tr},1,\boldsymbol{x}_{rc}}\, rc_{m_{tr},1,\boldsymbol{x}_{rc}} - rc^{\dagger}_{m_{tr},3,\boldsymbol{x}_{rc}}\, rc_{m_{tr},3,\boldsymbol{x}_{rc}}.$$

For example, the flip operator $\alpha^{\dagger}_{rc,1}$ destroys the ground state 1 of the receiver and transfers it in the upper state 2. The inversion operator, e.g. $\sigma_{rc,1}$, describes the difference between the occupation numbers of the upper state 2 and the lower ground state. Thus, the interaction Hamiltonian that describes the receiving phase is denoted by

$$H^{rec.}_{int}/\hbar = i g_{rc} \tag{84}$$

$$\Big[\sum_{tr,\boldsymbol{x}_i,\boldsymbol{k}_i,\boldsymbol{x}_j,\boldsymbol{k}_j,\boldsymbol{x}_{rc},\boldsymbol{x}_{ch}} \alpha^{\dagger}_{rc,1}\, nt_{m_{tr},\boldsymbol{x}_i,\boldsymbol{k}_i}\, nt_{m_{tr},\boldsymbol{x}_j,\boldsymbol{k}_j} ch^{\dagger}_{\boldsymbol{x}_{ch}}$$

$$-\sum_{tr,\boldsymbol{x}_i,\boldsymbol{k}_i,\boldsymbol{x}_j,\boldsymbol{k}_j,\boldsymbol{x}_{rc},\boldsymbol{x}_{ch}} \alpha_{rc,1}\, nt^{\dagger}_{m_{tr},\boldsymbol{x}_j,\boldsymbol{k}_j}\, nt^{\dagger}_{m_{tr},\boldsymbol{x}_i,\boldsymbol{k}_i} ch_{\boldsymbol{x}_{ch}}$$

$$+\sum_{tr,\boldsymbol{x}_i,\boldsymbol{k}_i,\boldsymbol{x}_j,\boldsymbol{k}_j,\boldsymbol{x}_{rc},\boldsymbol{x}_{ch}} \alpha^{\dagger}_{rc,2}\, nt_{m_{tr},\boldsymbol{x}_i,\boldsymbol{k}_i}\, nt_{m_{tr},\boldsymbol{x}_j,\boldsymbol{k}_j} ch^{\dagger}_{\boldsymbol{x}_{ch}}$$

$$-\sum_{tr,\boldsymbol{x}_i,\boldsymbol{k}_i,\boldsymbol{x}_j,\boldsymbol{k}_j,\boldsymbol{x}_{rc},\boldsymbol{x}_{ch}} \alpha_{rc,2}\, nt^{\dagger}_{m_{tr},\boldsymbol{x}_j,\boldsymbol{k}_j}\, nt^{\dagger}_{m_{tr},\boldsymbol{x}_i,\boldsymbol{k}_i} ch_{\boldsymbol{x}_{ch}}$$

$$+\sum_{tr,\boldsymbol{x}_i,\boldsymbol{k}_i,\boldsymbol{x}_j,\boldsymbol{k}_j,\boldsymbol{x}_{rc},\boldsymbol{x}_{ch}} \alpha^{\dagger}_{rc,3}\, nt_{m_{tr},\boldsymbol{x}_i,\boldsymbol{k}_i}\, nt_{m_{tr},\boldsymbol{x}_{tr_j},\boldsymbol{k}_{tr_j}} ch^{\dagger}_{\boldsymbol{x}_{ch}}$$

$$-\sum_{tr,\boldsymbol{x}_i,\boldsymbol{k}_i,\boldsymbol{x}_j,\boldsymbol{k}_j,\boldsymbol{x}_{rc},\boldsymbol{x}_{ch}} \alpha_{rc,3}\, nt^{\dagger}_{m_{tr},\boldsymbol{x}_j,\boldsymbol{k}_j}\, nt^{\dagger}_{m_{tr},\boldsymbol{x}_i,\boldsymbol{k}_i} ch_{\boldsymbol{x}_{ch}}\Big].$$

The corresponding coupling constant is called $g_{rc}$. We again emphasizes that the indices which represent the different molecules are not equal and we again require that the distances between a receiving molecule and two incoming neurotransmitters, as well as the **k**-space distance of wave number vectors, is governed by the following restrictions:

$$\left|\boldsymbol{x}_{rc} - \boldsymbol{x}_i\right| \le \varepsilon_{\boldsymbol{x}} \text{ resp. } \left|\boldsymbol{x}_{rc} - \boldsymbol{x}_j\right| \le \varepsilon_{\boldsymbol{x}};\ \left|\boldsymbol{k}_i - \boldsymbol{k}_j\right| \le \varepsilon_{\boldsymbol{k}};\ \forall\, i,j = 1,\ldots,n. \tag{85}$$

As well, the channel position (opening of the receiver) should be very close to the receiver position $\left|\boldsymbol{x}_{ch} - \boldsymbol{x}_{rc}\right| \le \varepsilon_{\boldsymbol{x}}$.

*Equations of motion of the reception phase*

The three equations of the flip operators are given by the following expressions:

$$\dot{\alpha}^{\dagger}_{rc,1} = -g_{rc} \sum_{tr,\boldsymbol{x}_i,\boldsymbol{k}_i,\boldsymbol{x}_j,\boldsymbol{k}_j,\boldsymbol{x}_{rc},\boldsymbol{x}_{ch},tr}\ \sigma_{rc,1} nt^{\dagger}_{m_{tr},\boldsymbol{x}_i,\boldsymbol{k}_i}\, nt^{\dagger}_{m_{tr},\boldsymbol{x}_j,\boldsymbol{k}_j} ch_{\boldsymbol{x}_{ch}} - \gamma_{rc,1}\alpha^{\dagger}_{rc,1}. \tag{86}$$

$$\dot{\alpha}^{\dagger}_{rc,2} = -g_{rc} \sum_{tr,\boldsymbol{x}_i,\boldsymbol{k}_i,\boldsymbol{x}_j,\boldsymbol{k}_j,\boldsymbol{x}_{rc},\boldsymbol{x}_{ch},tr}\ \sigma_{rc,2} nt^{\dagger}_{m_{tr},\boldsymbol{x}_i,\boldsymbol{k}_i}\, nt^{\dagger}_{m_{tr},\boldsymbol{x}_j,\boldsymbol{k}_j} ch_{\boldsymbol{x}_{ch}} - \gamma_{rc,2}\alpha^{\dagger}_{rc,2}. \tag{87}$$

$$\dot{\alpha}^{\dagger}_{rc,3} = -g_{rc} \sum_{tr,\boldsymbol{x}_i,\boldsymbol{k}_i,\boldsymbol{x}_j,\boldsymbol{k}_j,\boldsymbol{x}_{rc},\boldsymbol{x}_{ch},tr}\ \sigma_{rc,3} nt^{\dagger}_{m_{tr},\boldsymbol{x}_i,\boldsymbol{k}_i}\, nt^{\dagger}_{m_{tr},\boldsymbol{x}_j,\boldsymbol{k}_j} ch_{\boldsymbol{x}_{ch}} - \gamma_{rc,1}\alpha^{\dagger}_{rc,3}. \tag{88}$$

Here, we again indicate that in addition to the aforementioned restrictions (equation (84)) we demand the compliance of the two restrictions $\boldsymbol{x}_i = \boldsymbol{x}_q \pm \varepsilon_{\boldsymbol{x}}$, $\left|\boldsymbol{k}_i - \boldsymbol{k}_q\right| \le \varepsilon_{\boldsymbol{k}}$, (equivalent for $\boldsymbol{x}_j$ and $\boldsymbol{k}_j$).

The significance of the equations (86) − (88) can be already elucidated by the first expression (86). The transition from state 1 to state 2 is initiated by the increase of the occupation number of state 2 and the decrease of the occupation number of state 1 ($\sigma_{rc,1}$). This is equivalent to the creation of two neurotransmitters in the very close vicinity of the receptor, and the annihilation of the channel because it is

closed.

The dynamics of the three inversion operators are described by the following expressions:

$$\dot{\sigma}_{rc,1} = 2g_{rc}\sum_{tr,\boldsymbol{x}_i,\boldsymbol{k}_i,\boldsymbol{x}_j,\boldsymbol{k}_j,\boldsymbol{x}_{rc},\boldsymbol{x}_{ch}} \Big[\alpha^{\dagger}_{rc,1} nt_{m_{tr},\boldsymbol{x}_i,\boldsymbol{k}_i}\, nt_{m_{tr},\boldsymbol{x}_j,\boldsymbol{k}_j} ch^{\dagger}_{x_{ch}} + \alpha_{rc,1} nt^{\dagger}_{m_{tr},\boldsymbol{x}_j,\boldsymbol{k}_j}\, nt^{\dagger}_{m_{tr},\boldsymbol{x}_i,\boldsymbol{k}_i} ch_{\boldsymbol{x}_{ch}}\Big] - \gamma_{rc,1}\sigma^{\dagger}_{rc,1}. \quad (89)$$

$$\dot{\sigma}_{rc,2} = 2g_{rc}\sum_{tr,\boldsymbol{x}_i,\boldsymbol{k}_i,\boldsymbol{x}_j,\boldsymbol{k}_j,\boldsymbol{x}_{rc},\boldsymbol{x}_{ch}} \Big[\alpha^{\dagger}_{rc,2} nt_{m_{tr},\boldsymbol{x}_i,\boldsymbol{k}_i}\, nt_{m_{tr},\boldsymbol{x}_j,\boldsymbol{k}_j} ch^{\dagger}_{x_{ch}} + \alpha_{rc,2} nt^{\dagger}_{m_{tr},\boldsymbol{x}_j,\boldsymbol{k}_j}\, nt^{\dagger}_{m_{tr},\boldsymbol{x}_i,\boldsymbol{k}_i} ch_{\boldsymbol{x}_{ch}}\Big] - \gamma_{rc,2}\sigma^{\dagger}_{rc,2}. \quad (90)$$

$$\dot{\sigma}_{rc,3} = 2g_{rc}\sum_{tr,\boldsymbol{x}_i,\boldsymbol{k}_i,\boldsymbol{x}_j,\boldsymbol{k}_j,\boldsymbol{x}_{rc},\boldsymbol{x}_{ch}} \Big[\alpha^{\dagger}_{rc,3} nt_{m_{tr},\boldsymbol{x}_i,\boldsymbol{k}_i}\, nt_{m_{tr},\boldsymbol{x}_j,\boldsymbol{k}_j} ch^{\dagger}_{x_{ch}} + \alpha_{rc,3} nt^{\dagger}_{m_{tr},\boldsymbol{x}_j,\boldsymbol{k}_j}\, nt^{\dagger}_{m_{tr},\boldsymbol{x}_i,\boldsymbol{k}_i} ch_{\boldsymbol{x}_{ch}}\Big] - \gamma_{rc,3}\sigma^{\dagger}_{rc,3}. \quad (91)$$

In the following, we again consider the first equation (86) to outline the behavior of an inversion operator. The change of this inversion operator (initial state s = 1) is governed by the flipping of state 1 to state 2, the annihilation of two neurotransmitters in the direct environment of the receptor and the creation of an ion channel. Alternatively (initial state s = 2), the inverse process occurs.

The creation of the inversion operators, the annihilation of a neurotransmitter and the creation of a channel operator regulate the dynamics of a created neurotransmitter operator.

$$\dot{nt}^{\dagger}_{m_{tr},\boldsymbol{x}_q,\boldsymbol{k}_q} = -g_{rc}\sum_{tr,\boldsymbol{x}_j,\boldsymbol{k}_j,\boldsymbol{x}_{rc},\boldsymbol{x}_{ch}} \left(\alpha^{\dagger}_{rc,1} + \alpha^{\dagger}_{rc,2} + \alpha^{\dagger}_{rc,3}\right) nt_{m_{tr},\boldsymbol{x}_j,\boldsymbol{k}_j} ch^{\dagger}_{x_{ch}} - \gamma_{nt} nt^{\dagger}_{m_{tr},\boldsymbol{x}_q,\boldsymbol{k}_q}. \quad (92)$$

$$\dot{ch}^{\dagger}_{x_q} = -g_{rc}\sum_{tr,\boldsymbol{x}_i,\boldsymbol{k}_i,\boldsymbol{x}_j,\boldsymbol{k}_j,\boldsymbol{x}_{rc}} \left(\alpha_{rc,1} + \alpha_{rc,2} + \alpha_{rc,3}\right) nt^{\dagger}_{m_{tr},\boldsymbol{x}_i,\boldsymbol{k}_i}\, nt^{\dagger}_{m_{tr},\boldsymbol{x}_j,\boldsymbol{k}_j} - \gamma_{ch} ch^{\dagger}_{x_q}. \quad (93)$$

The selection of one particular flip operator out of the three flip operators is determined by the given initial state. If we chose $s = 2$ as the initial state then we have only to consider $\alpha_{rc,1}$ in equation (92). The state of the receiver makes a transition from $s = 2$ to $s = 1$ (regular transition cycle) and two neurotransmitters are also created.

The temporal spatial and momentum density of arriving neurotransmitters reads

$$\frac{d}{dt}\left(nt^{\dagger}_{m_{tr},\boldsymbol{x}_q,\boldsymbol{k}_q}\, nt_{m_{tr},\boldsymbol{x}_q,\boldsymbol{k}_q}\right) = -g_{rc}\sum_{tr,\boldsymbol{x}_j,\boldsymbol{k}_j,\boldsymbol{x}_{rc},\boldsymbol{x}_{ch}} \Big[\alpha^{\dagger}_{rc,1} nt_{m_{tr},\boldsymbol{x}_j,\boldsymbol{k}_j}\, nt_{m_{tr},\boldsymbol{x}_q,\boldsymbol{k}_q} ch^{\dagger}_{tr,x_{ch}} + \alpha_{rc,1} nt^{\dagger}_{m_{tr},\boldsymbol{x}_j,\boldsymbol{k}_j} nt^{\dagger}_{m_{tr},\boldsymbol{x}_q,\boldsymbol{k}_q}\, ch_{x_{ch}} + \alpha^{\dagger}_{rc,2} nt_{m_{tr},\boldsymbol{x}_j,\boldsymbol{k}_j}\, nt_{m_{tr},\boldsymbol{x}_q,\boldsymbol{k}_q} ch^{\dagger}_{tr,x_{ch}} + \alpha_{rc,2} nt^{\dagger}_{m_{tr},\boldsymbol{x}_j,\boldsymbol{k}_j}\, nt^{\dagger}_{m_{tr},\boldsymbol{x}_q,\boldsymbol{k}_q} ch_{x_{ch}} \alpha^{\dagger}_{rc,3} nt_{m_{tr},\boldsymbol{x}_j,\boldsymbol{k}_j}\, nt_{m_{tr},\boldsymbol{x}_q,\boldsymbol{k}_q} ch^{\dagger}_{tr,x_{ch}} + \alpha_{rc,3}\, nt^{\dagger}_{m_{tr},\boldsymbol{x}_j,\boldsymbol{k}_j}\, nt^{\dagger}_{m_{tr},\boldsymbol{x}_q,\boldsymbol{k}_q} ch_{x_{ch}}\Big] - \gamma_{nt} nt^{\dagger}_{m_{tr},\boldsymbol{x}_q,\boldsymbol{k}_q}\, nt_{m_{tr},\boldsymbol{x}_q,\boldsymbol{k}_q}. \quad (94)$$

Figure 7 represents by a phase diagram the temporal dependence of the real part (red) and imaginary part (blue) of the operator $\alpha^{\dagger}_{rc,1}$ (equation (86)), $nt^{\dagger}_{m_{tr},\boldsymbol{x}_q,\boldsymbol{k}_q}$ (equation (92)) and $ch^{\dagger}_{x_q}$ (equation (93)).

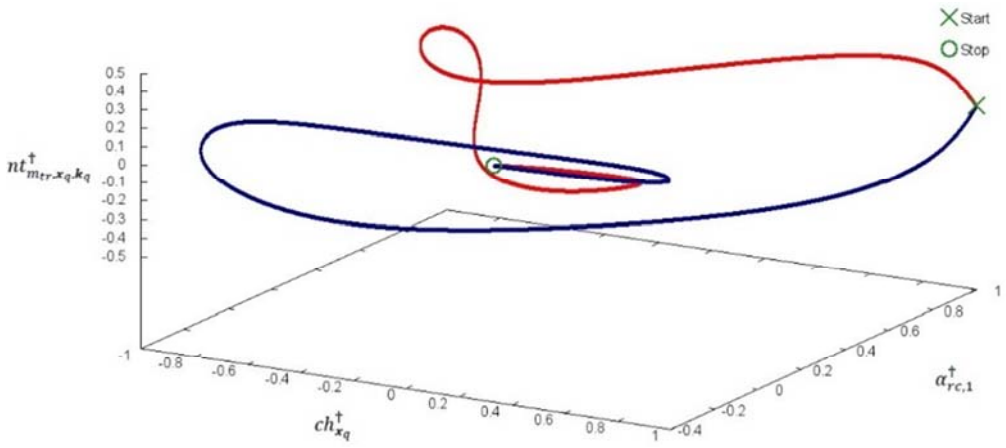


***Figure 7.*** *Graphical representation of the temporal behavior of the real part (red) and imaginary part (blue) of the three operators $\alpha^{\dagger}_{rc,1}$ (equation (86), $nt^{\dagger}_{m_{tr},\boldsymbol{x}_q,\boldsymbol{k}_q}$ (equation (92)), and $ch^{\dagger}_{x_q}$ (equation (93). The common damping constant is set to $\gamma = 0.05$.*

Figure 8 describes the temporal trajectories of the density of neurotransmitters during the reception phase (equation (94)), where the real (red) and the imaginary (blue) part are separated.

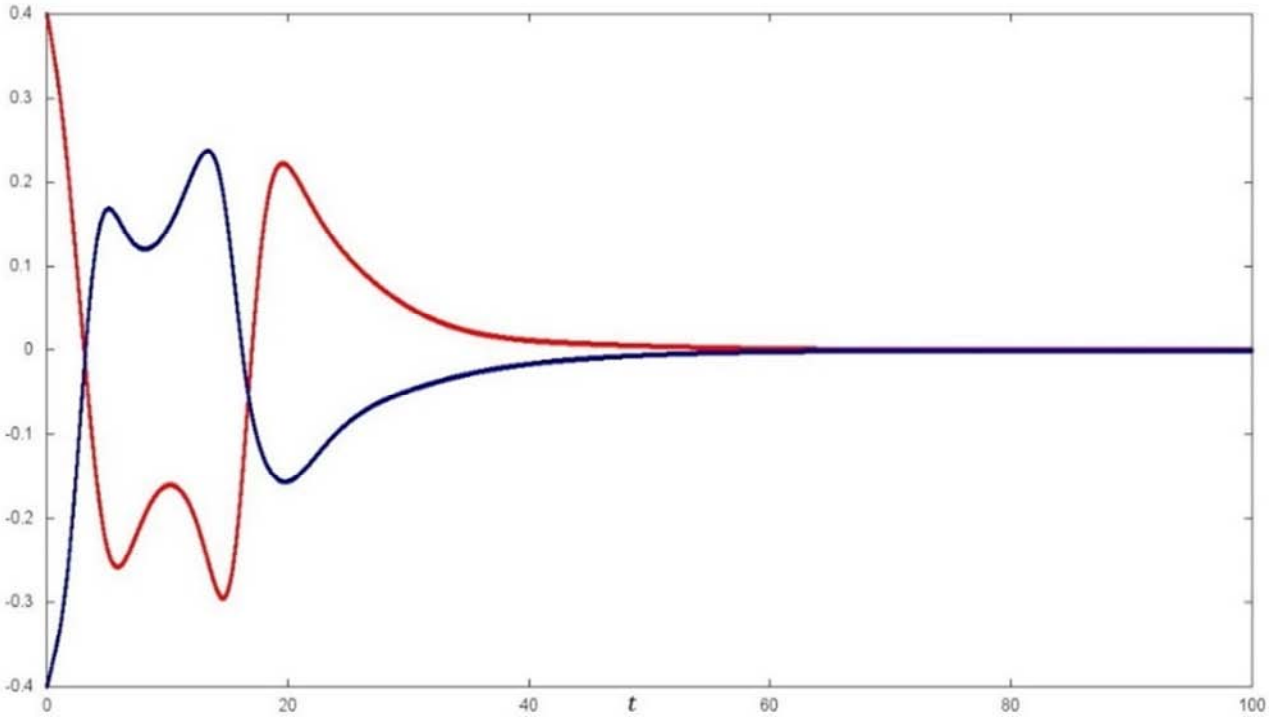


***Figure 8.*** *Density of the impinging neurotransmitters in the timespan of the reception phase (equation (94)). The real part is shown in red; the imaginary part is marked by blue. The damping constant is $\gamma_{nt}$ =0.05, the coupling constant is $g_{rec} = 0.1$. The scale of time axis is characteristic for the release process, here the numerical value 100 corresponds approximately 1ms.*

The dynamics of the three receivers is characterized by their strong coupling:

$$\dot{r}c^{\dagger}_{m_{tr},1,\boldsymbol{x}_{rc}} = g_{rc}\sum\nolimits_{tr,\boldsymbol{x}_i,\boldsymbol{k}_i,\boldsymbol{x}_j,\boldsymbol{k}_j,\boldsymbol{x}_{rc},\boldsymbol{x}_{ch}} (rc^{\dagger}_{m_{tr},3,\boldsymbol{x}_{rc}} - rc^{\dagger}_{m_{tr},2,\boldsymbol{x}_{rc}})\, nt_{m_{tr},\boldsymbol{x}_i,\boldsymbol{k}_i}\, nt_{m_{tr},\boldsymbol{x}_j,\boldsymbol{k}_j} ch^{\dagger}_{\boldsymbol{x}_{ch}} - \gamma_{rc} rc^{\dagger}_{m_{tr},1,\boldsymbol{x}_{rc}}. \quad (95)$$

$$\dot{r}c^{\dagger}_{m_{tr},2,\boldsymbol{x}_{rc}} = g_{rc}\sum\nolimits_{tr,\boldsymbol{x}_i,\boldsymbol{k}_i,\boldsymbol{x}_j,\boldsymbol{k}_j,\boldsymbol{x}_{rc},\boldsymbol{x}_{ch}} (rc^{\dagger}_{m_{tr},1,\boldsymbol{x}_{rc}} - rc^{\dagger}_{m_{tr},3,\boldsymbol{x}_{rc}})\, nt_{m_{tr},\boldsymbol{x}_i,\boldsymbol{k}_i}\, nt_{m_{tr},\boldsymbol{x}_j,\boldsymbol{k}_j} ch^{\dagger}_{\boldsymbol{x}_{ch}} - \gamma_{rc} rc^{\dagger}_{m_{tr},2,\boldsymbol{x}_{rc}}. \quad (96)$$

$$\dot{r}c^{\dagger}_{m_{tr},3,\boldsymbol{x}_{rc}} = g_{rc}\sum\nolimits_{tr,\boldsymbol{x}_i,\boldsymbol{k}_i,\boldsymbol{x}_j,\boldsymbol{k}_j,\boldsymbol{x}_{rc},\boldsymbol{x}_{ch}} (rc^{\dagger}_{m_{tr},2,\boldsymbol{x}_{rc}} - rc^{\dagger}_{m_{tr},1,\boldsymbol{x}_{rc}})\, nt_{m_{tr},\boldsymbol{x}_i,\boldsymbol{k}_i}\, nt_{m_{tr},\boldsymbol{x}_j,\boldsymbol{k}_j} ch^{\dagger}_{\boldsymbol{x}_{ch}} - \gamma_{rc} rc^{\dagger}_{m_{tr},3,\boldsymbol{x}_{rc}}. \quad (97)$$

The solutions of these three coupled differential equations are required to describe the time-dependent density of a receiver which is in the state "unoccupied and closed" (state 1). The corresponding result is given by

$$\frac{d}{dt}\left(rc^{\dagger}_{m_{tr},1,\boldsymbol{x}_{rc}}\, rc_{m_{tr},1,\boldsymbol{x}_{rc}}\right) = -g_{rc}\sum\nolimits_{tr,\boldsymbol{x}_j,\boldsymbol{k}_j,\boldsymbol{x}_{rc},\boldsymbol{x}_{ch},tr}\Big[\alpha^{\dagger}_{rc,1} nt_{m_{tr},\boldsymbol{x}_i,\boldsymbol{k}_i}\, nt_{m_{tr},\boldsymbol{x}_j,\boldsymbol{k}_j} ch^{\dagger}_{\boldsymbol{x}_{ch}} - \alpha_{rc,1} nt^{\dagger}_{m_{tr},\boldsymbol{x}_j,\boldsymbol{k}_j}\, nt^{\dagger}_{m_{tr},\boldsymbol{x}_i,\boldsymbol{k}_i} ch_{\boldsymbol{x}_{ch}}\Big] - \gamma_{rc} rc^{\dagger}_{m_{tr},1,\boldsymbol{x}_{rc}}\, rc_{m_{tr},1,\boldsymbol{x}_{rc}}. \quad (98)$$

If we compare this result with that one we obtained for the three inversion operators (equations (89) – (91)) then it will be obvious that the right hand side of equation (98) is formed by the sum of the expressions of the previously mentioned equations. Figure 9 illustrates the time dependent density of a receptor in state $s = 1$ (equation (98)) whilst the reception phase, where again the real part (red) and the imaginary part (blue) are together outlined.

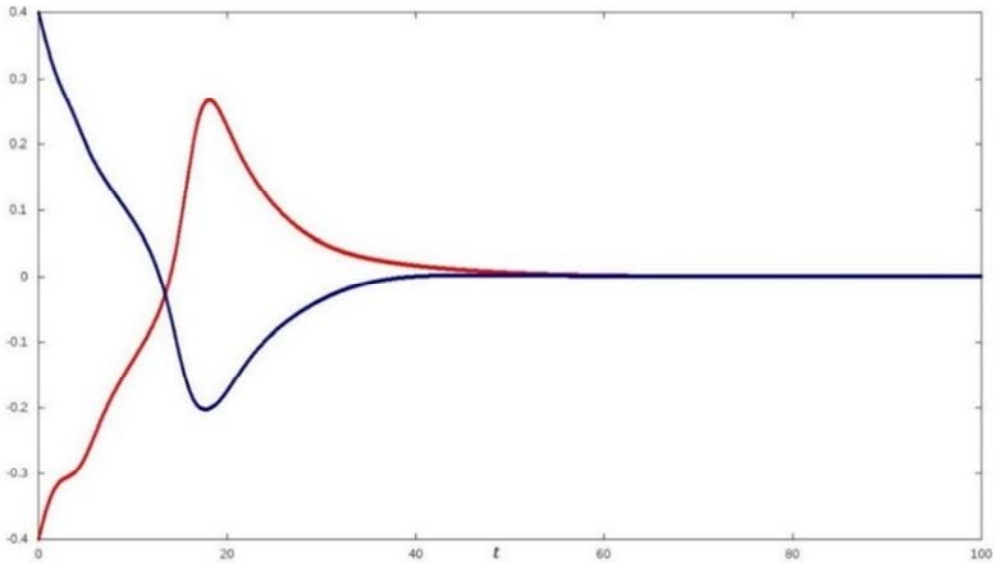


***Figure 9.*** *Depiction of the temporal variations of the density of receptors (equation (98)). The real part is marked by red; the imaginary part is labeled by blue. The damping constant is set to $\gamma_{rc} = 0.05$; the coupling constant takes the value $g_{rc} = 0.1$. The scale of time axis is characteristic for the reception phase, where the numerical value100 corresponds approximately 1ms.*

# 5. Conclusions

In our approach, several dominant quantum effects characterize the whole transmission cycle in chemical synapses. First, the interactions of all involved molecules of the five modelled, principal phases are specified by the Hamiltonians, which model the simultaneous reciprocal actions of the creation operators and corresponding annihilation operators. This interplay defines the resulting molecular dynamics.

Second, the molecular dynamics of the loading process is characterized by a competitive balancing between loading and unloading. The transport of neurotransmitters along axonal microtubules is regarded as an efficient replacement of the diffusion process. The synchronization of the vesicle transport is done by the stepwise motion control of the load carrying molecular robots. Third, the release of the neurotransmitters can also be represented as the multiple outgoing of plane matter waves, which superposes to wave packets, where their group velocities correspond to particle velocities.

Fourth, the transmissions through the cleft is represented by three different approaches: multiple scattering, quantum diffusion and *n*-particle system. In the first attempt, we use Green´s functions to calculate the probability of finding the final location of manifold scattered transmitters. Similar calculations can be performed with respect to the final *k*-value by the declaration of Green´s functions in the *k*-space. The quantum based diffusion mainly operates in the particle representation of the QFT, thus all densities, flows, transition elements, density matrix, etc. are calculated by the use of corresponding number operators and continuity equations. Hereby, we regard the quantum information, which is generated with the aid of the density matrix as one of the basic biological features that is relevant for the interconnections of neural populations (plasticity). The third approach uses the n-particle system, which obey the Schrödinger equation to establish the combination of the configuration space and the particle space. Hereby, we calculate the amplitude whose squared modulus give us the probability to find at n different positions at the same time *t*, $n_1$ particles with energy $E_1$, etc.

Fifth, the receptors can undergo quantum-based transitions into three different states, where these transitions are subjected to the rate of the incoming neurotransmitters. The interplay between sender and receiver is also governed by the loss rate of the neurotransmitters that directly influence the resulting gain.

In summary, this contribution shows the entry point of a path, which may ends up with the proved statement that quantum processes occur in the brain. One important, still open question is, do coherent states (matter waves) exist in the brain and can we therefore observe interference effects by experiments (whether in vitro or in vivo).

# Acknowledgments

The research leading to these results has received funding from the European Union HBP FETFLAGSHIP project in Horizon 2020 (No. 720270, SGA1, SP 10). We also express our gratitude to Dr. B. Schenke for his extensive, numerical support of this contribution. Moreover, we thank Mr. C. Price for his steady encouragement to finish this contribution.

# References

[1] Abeles M., Diesmann M, Flash T, Geisel T, Herrmann J M, Teicher M (2013). *Compositionality in Neural Control: An Interdisciplinary Study of Scribbling Movements in Primates*. Front. Comput. Neurosci. 7 (103): 10.3389/fncom.2013.00103.

[2] Albers B, Johnson A, Lewis J, Raff M, Roberts K, Walter P (2008). *Molecular Biology of the Cell*. 5th ed., New York, Garland Science.

[3] Arndt M, Nairz O, Vos–Andrae J, Keller C, van der Zouw G, and Zeilinger A (1999). *Wave-particle duality of $C_{60}$ molecules*. Letters to Nature 401, 680-682; doi: 10.1038/44348.

[4] Bear FB, Connors BW, Paradiso MA, (2015). *Principles of Neuroscience*. 4th ed. Philadelphia, Wolters Kluwer.

[5] Beck, F., Eccles, J., (2003). *Quantum Processes in the Brain*. Neural Basis of consciousness. Proc Nat Acad Sci (49) (2003): 141.

[6] Bardeen J, Cooper L, and Schrieffer R (1957). *Theory of Superconductivity*. Phys. Rev. 108, Iss. 5. doi: http//dx.doi.org/10.1103/PhysRev.108.1175.

[7] Bjorken, J. and Drell, S, (1965). *Relativistic Quantum Fields*. New York, McGraw–Hill.

[8] Dyan P and Abbott LF (2005). *Theoretical Neuroscience*. Second ed., Cambridge, The MITPress.

[9] Bruce NJ, Kokh DB, Ozboyaci M and Wade R C (2015). *Modelling of solvation effects for Brownian dynamics simulation of biomolecular recognition.* In Computational Trends in Solvation and Transport in Liquids. Lecture Notes, volume 28 of IAS Series, (2015), 259-280. Eds. Sutmann G et al.: Schriften des Forschungszentrums Juelich.

[10] Einstein, A. (1905). *Über die von der molekularkinetischen Theorie der Wärme geforderte Bewegung von in ruhenden Flüssigkeiten suspendierten Teilchen*. Annalen der Physik, 322 (8), 549–560. doi: 10.1002/andp.19053220806.

[11] Feynman R P (1955). *Progress in low Temperature Physics*. Vol. 1. Amsterdam, North–Holland. Chapter II: *Application of Quantum Mechanics to Liquid Helium*. doi: 10.1016/S0079–6417(08)60077–3.

[12] Feynman RP and Hibbs AR (2005). *Quantum Mechanics and Path Integrals*. Emended edition, New York, Mc Graw-Hill.

[13] Gerstner Wand Kistler W. (2011). *Spiking Neuron Models*. Second ed., Cambridge University Press.

[14] Gerstner W, Kistler W, Naud R, and Paninski L (2014). *Neural Dynamics: From Single Neurons to Networks and Models of Cognition*. Cambridge, Cambridge University Press.

[15] Hagan, Sc., Hameroff, St., and Tuszynski, J., (2014). *Quantum Computation in Brain Micro- tubules: Decoherence and biological Feasibility*. Physical Review E65.6 (2002): 061901.

[16] Haken H (2003). *Quantum Field Theory of Solids*. Amsterdam, Elsevier.

[17] Haken H, Levi P (2012). *Synergetic Agents–Classical and Quantum. From Multi-Robot Systems to Molecular Robotics*. Weinheim, Wiley-VCH.

[18] Haken H, Wolf H Ch (2006). *Molekülphysik und Quantenchemie*, 5. Auflage. Berlin, Springer Verlag.

[19] Helias M, Rotter St, Gewaltig M-O and Dismann M (2008). *Structural Plasticity Controlled by Calcium Based Correlation Detection.* Frontier in Computational Neuroscience, doi: 10.3389/neuro.10.007.2008.

[20] Huelga, S. F., Plenio, M. B., (2011). *Quantum Dynamics of bio-molecular Systems in noisy Environments.* 22nd Solvay Conference in Chemistry, Procedia Chemistry 00(2011) 1-10., www.sciencedirect.com

[21] Kandel ER, Schwartz J, H., Jessel Th M (Eds.), (2012). *Essentials of Neural Science and Behavior*. 5th ed., Appleton, open library Appleton & Lange.

[22] Kurtsiefer Ch, Pfau T, Mlynek J (1997). *Experimental Determination of the Motional Wigner Function of a Helium Atom*. Nature 386, 150.

[23] Lambert N, Chen YN, Li CM, Chen GY, Nori F (2013). *Quantum Biology*. Nature Physics 9, 10-18, doi: 10.138/nphys2474.

[24] Levi, P (2015). *Molecular Quantum Robotics: Particle and Wave Solutions, illustrated by "Leg-over-Leg" Walking along Microtubules*. Frontiers in Neurorobotics, May 2015, Vol. 9, Article 2. doi: 10.3389/fnbot.2015.00002.

[25] Levine IN (2013). *Quantum Chemistry*. New Jersey, Prentice Hall.

[26] Lurié D (1968). *Particles and Fields*. New York, John Wiley & Sons.

[27] Markram H (2006). *The Blue Brain Project*. Nature Reviews Neuroscience 7, 153 – 160. PMID 16429124.

[28] Myung J, Hong S, de Woskin D, de Schutter E, Forger DB, Takumi T (2015). *GaBa–mediated repulsive coupling between circadian clock neurons in the SCN encodes seasonal time*. Proc Natl Acad Sci USA, 112 (29): E3920-9. doi: 10.1073/pnas.

[29] PAPETS: *Phonon-Assisted Processes for Energy Transfer and Sensory*, (2016). EU FP7 FET project.

[30] Plesser H, Diesmann M., Gewaltig M-O, Morrison A (2015), *NEST the neural simulation tool*. Encyclopedia of computational neuroscience, eds. Jaeger, D., Jung, R., 1849 – 1852, New York, Springer Verlag.

[31] Onsager L (1949). *Statistical Hydrodynamics*. Nuovo Cimento, Vol. 6, 279 – 287.

[32] Roux B. (2011). *Molecular Machines*. Singapore, World Scientific Publishing Co.

[33] Seeman NC (2004). *Nanotechnology and the double helix.* Scientific American 290 (6), 64–76. doi. 10.1038/scientificamerican0604–64.

[34] Szabo A, Ostlund NS (1966). *Modern Quantum Chemistry*. New York, Dover Books.

[35] Weinberg S (2005). *The Quantum Theory of Fields*, Vol. I, II, III. Cambridge, Cambridge University Press.

[36] Weinberg S (2013). *Lectures on Quantum Mechanics*. Cambridge, Cambridge University Press.